Mon. Not. R. Astron. Soc. **396,** 1709–1731 (2009) doi:10.1111/j.1365-2966.2009.14855.x

# Seismological studies of ZZ Ceti stars – II. Application to the ZZ Ceti class

B. G. Castanheira[1,2★] and S. O. Kepler[1]

[1]*Departamento de Astronomia, Universidade Federal do Rio Grande do Sul, Av. Bento Gonçalves 9500 Porto Alegre 91501-970, RS, Brazil*
[2]*Institut für Astronomie, Türkenschanzstr. 17, A-1180 Wien, Austria*

Accepted 2009 April 1. Received 2009 March 30; in original form 2008 August 27

**ABSTRACT**

We used the detected pulsation modes and adiabatic pulsation models to do seismology of the class of ZZ Ceti stars and measure the H layer mass for 83 stars. We found the surface hydrogen layer to be within the range $10^{-9.5} \geq M_{\rm H}/M_* \geq 10^{-4}$, with an average of $M_{\rm H}/M_* = 10^{-6.3}$, which is thinner than the predicted value of $M_{\rm H}/M_* = 10^{-4}$, indicating that the stars lose more mass during their evolution than previously expected. These results are preliminary and do not include the possible effects of realistic C/O profiles on the fits.

**Key words:** stars: individual: ZZ Ceti stars – stars: variables: other – white dwarfs.

## 1 INTRODUCTION

White dwarfs are the final evolutionary stage of almost all stars (95–98 per cent; e.g. Fontaine, Brassard & Bergeron 2001). Their evolution is basically dominated by cooling. As they cool down, they pass through three distinct instability strips: around $T_{\rm eff} \sim 100\,000$ K (the DOV or GW Vir stars), around $T_{\rm eff} \sim 25\,000$ K (the DBV stars) and around $T_{\rm eff} \sim 12\,000$ K (the DAV or ZZ Ceti stars). The element that drives pulsation is different in each strip: carbon and/or oxygen for DOVs, helium for DBVs and hydrogen for DAVs.

The study of stellar pulsations, i.e. asteroseismology, is the most powerful tool to study stellar interiors and evolution. Pulsations probe the internal structure of the stars, as every mode is, in principle, an independent measurement of the stellar structure. Even from just a few pulsation modes we can estimate fundamental stellar properties, such as stellar mass (Castanheira & Kepler 2008, hereafter Paper I). Moreover, if a large number of modes are observed, the structure of the star can be determined in detail (e.g. Metcalfe 2005).

As multiperiodic pulsators, pulsating white dwarfs allow detailed information about their structure and evolution. Through modelling, the shape of the light curves can provide the structure of the convective zone (Montgomery 2005a). In addition, the excited modes allow us to measure the interior chemical composition, and the period spacing provides reliable stellar mass (Costa 2004; Córsico et al. 2008) with a precision up to $0.02\,{\rm M}_{\odot}$. It is important to emphasize that the seismological uncertainties are totally dominated by the models, not due to observational constraints. Asteroseismology also allows us to constrain the value of the C($\alpha$, $\gamma$)O cross-section (Metcalfe 2005), which cannot be measured in any terrestrial laboratory. Cooling times for white dwarfs can be directly measured from the rate of change of the pulsation periods (Kepler et al. 2005a), and these cooling times can be used to estimate the age of the Galaxy components (e.g. Hansen & Liebert 2003). Periodic modulations of the times of arrival of the pulsations would reveal the presence of planets around these stars (Winget et al. 2003; Mullally et al. 2008). Finally, pulsating white dwarfs are important to study the physics at high densities: crystallization (e.g. Kanaan et al. 2005), neutrino cooling (Winget et al. 2004) and axion emission (Córsico et al. 2001; Bischoff-Kim, Montgomery & Winget 2008).

In Paper I, we focus our studies on a few of the coolest known pulsating instability strip, the ZZ Ceti stars. Observationally, the star starts to pulsate when the effective temperatures are slightly above 12 000 K, showing a few short periods and small-amplitude modes, defining the so-called blue edge of the ZZ Ceti instability strip. The standard picture is that pulsations start when the partial ionization zone of hydrogen (H) deepens into the envelope. As the stars cool down, the depth of the convective zone increases, as well as its size. Around 11 500 K, there is a sudden deepening of the convection zone in the models; the observed pulsations change in character, with more modes with long and higher amplitudes excited. At temperatures slightly lower than 11 000 K, the stars stop to pulsate, defining the red edge of the ZZ Ceti instability strip. The high amplitudes observed on the cool part of the strip decrease, consistent with an increase of the depth of the convective zone (Brickhill 1991; Mukadam et al. 2006).

Mukadam et al. (2006) calculated the weighted mean period (WMP), by weighting each observed period ($P$) with the corresponding amplitude ($A$), as

$$\mathrm{WMP} = \frac{\sum_i P_i A_i}{\sum_i A_i}. \quad (1)$$

Despite the extreme relevance of this work, we used a definition of WMP, where the weights come from the relation between pulsation energy and amplitude squared ($E \propto A^2$),

$$\langle P \rangle = \frac{\sum_i P_i A_i^2}{\sum_i A_i^2}. \quad (2)$$

In Paper I, we have built and explored an extensive seismological model grid for pulsating white dwarfs with hydrogen-dominated

★E-mail: castanheira@astro.univie.ac.at

atmospheres, the ZZ Ceti stars. We varied four quantities: $T_{\rm eff}$, $M$, $M_{\rm H}$ and $M_{\rm He}$. Because the ZZ Cetis pulsate with only a few modes, we decided to use a fixed homogeneous C/O 50:50 core to decrease the number of model parameters, but still be consistent with the reaction rate uncertainty. Comparing our simple profile to Salari's, we show that the price paid for this choice is that the He layer mass determinations are uncertain. Our results do not include the possible effect of realistic C/O profiles on the fits.

In our fitting approach, we choose to weight the periods by pulsation energy, which is proportional to the amplitude squared ($A^2$), minimizing the $S$, which is proportional to the standard $\chi^2$:

$$S = \sum_{i=1}^{n} \sqrt{\frac{[P_{\rm obs}(i) - P_{\rm model}]^2 \times w_{\rm P}(i)}{\sum_{i=1}^{n} w_{\rm P}(i)}}, \quad (3)$$

where $n$ is the number of observed periods ($P$) and $w_{\rm P}$ is the relative uncertainty in period. The normalization is chosen to express $S$ in seconds.

Even though our adiabatic model grid does not provide theoretical amplitudes, we used the observed relative amplitudes to weight our fits: $w_{\rm P} \propto A^2$. This procedure guarantees that the fit will always be dominated by the higher amplitude modes, which are also a temperature discriminator. As we are calculating adiabatic models, the periods themselves are not dependent on temperature, to first order, but which mode is excited (e.g. Mukadam et al. 2006). In this paper, we present the comparison to our model grid to all known ZZ Ceti stars, using the technique to study the group properties.

## 2 SEISMOLOGY OF ZZ CETI STARS BY GROUPS

The motivation of grouping the stars is to use the similarities to lower the uncertainties. For stars with similar temperature, mass and excited modes, it is reasonable to expect that their internal structure would be similar as well. Our approach is akin to having several independent measurements for one particular star.

Our first task was the identification of all periodicities known for all ZZ Ceti stars. We re-analysed the light curves of the stars observed at the 2.1-m telescope at the McDonald Observatory for other projects, like the search for new ZZ Ceti stars conducted by Mukadam et al. (2004), Mullally et al. (2005) and Castanheira et al. (2006), and the search for extra-solar planets orbiting ZZ Ceti stars with stable modes (Mullally et al. 2008). We did the same for the light curves of the new ZZ Ceti stars discovered with the 4.1-m telescope SOuthern Astrophysical Research (SOAR) and the 1.6-m telescope at the Observatório Pico dos Dias (Kepler et al. 2005b; Castanheira et al. 2006, 2007). The other ZZ Ceti periods were obtained from the literature.

We separate the blue edge ZZ Ceti stars according to the excited mode with highest amplitude. We compared the observed modes with our model grid in the same way as for the individual stars, described in Paper I, i.e. we minimize $S$, defined in equation (3), weighting each period with the observed amplitude squared. We are searching for common properties to characterize a particular group; each group is a specific evolutionary stage in the white dwarf cooling.

Of the 143 known ZZ Ceti stars to date, 83 have been selected from the Sloan Digital Sky Survey (SDSS) sample. SDSS spectra for $g \leq 18$ stars have signal-to-noise ratio (S/N) $\sim 30$, and therefore temperature and mass are reasonably well determined (Kepler et al. 2006). However, this is not the case for stars fainter than $g = 18$. Bergeron et al. (1995, 2004) followed by Gianninas, Bergeron & Fontaine (2005) discussed that only with spectra S/N $\geq$ 70 one can obtain precise temperature ($\Delta T_{\rm eff} \simeq 300$ K) and gravity determinations ($\Delta \log g \simeq 0.1$). Their uncertainties are the external estimates, obtained by fitting the H line profiles of duplicate spectra. This is not the same uncertainty quoted for the SDSS stars, as most of them have only one spectrum; the published uncertainties are the internal values, obtained by fitting the whole spectrum, combined with colours (see Eisenstein et al. 2006 for detailed explanation). The external uncertainties by comparing duplicated SDSS spectra are of the order of 300 K (Kleinman et al. 2004; Eisenstein et al. 2006; Kepler et al. 2007). Kepler et al. (2006), comparing SDSS and *Gemini* (S/N $\geq$ 70) spectra, found $\Delta T_{\rm eff} \simeq 320$ K, systematically lower in SDSS, and $\Delta \log g \simeq 0.24$ dex, systematically larger in SDSS.

Koester & Allard (2000) used ultraviolet spectra instead of optical, which results in a higher mass uncertainty, but much better temperature determination. An additional external uncertainty comes from the differences in the model grids from Kiel (e.g. Koester et al. 2001) and Montreal (e.g. Bergeron et al. 2004), which is around 200 K, using a similar line profile fitting technique (Bergeron et al. 2004).

Like in Paper I, we used the external temperature and mass determinations as a guide for the search of the best among all the possible families of seismological solutions.

### 2.1 Main period ∼212 s

In Paper I, we analysed G117−B15A and G185−32, both with main mode ∼215 s, similar to the members of this group. In Table 1, we list the observed modes, spectroscopic temperature and mass determinations for the other stars with main mode around 212 s, considering 3 s in period corresponds to about 300 K in effective temperature, the average uncertainty from spectroscopic determinations.

**Table 1.** List of ZZ Ceti stars with main excited mode near $P \sim 212$ s.

| Star | Modes (s) | Amp (mma) | $T_{\rm eff}$ (K) | $M$ ($M_\odot$) | Reference |
|---|---|---|---|---|---|
| R 548 | 212.950 | 5.4 | 11 990 ± 200 | 0.59 ± 0.03 | Bergeron et al. (2004) |
| | 274.512 | 3.5 | 11 830 ± 150 | 0.50 ± 0.07 | Koester & Allard (2000) |
| | 333.64 | 1.3 | | | |
| | 318.07 | 1.1 | | | |
| | 187.28 | 0.9 | | | |
| G132−12 | 212.7 | 4.3 | 12 080 ± 200 | 0.57 ± 0.02 | (Gianninas, Bergeron & Fontaine 2006) |
| WD J2153−0731 | 210.2 | 5.6 | 11 930 ± 130 | 0.65 ± 0.04 | Castanheira et al. (2006) |

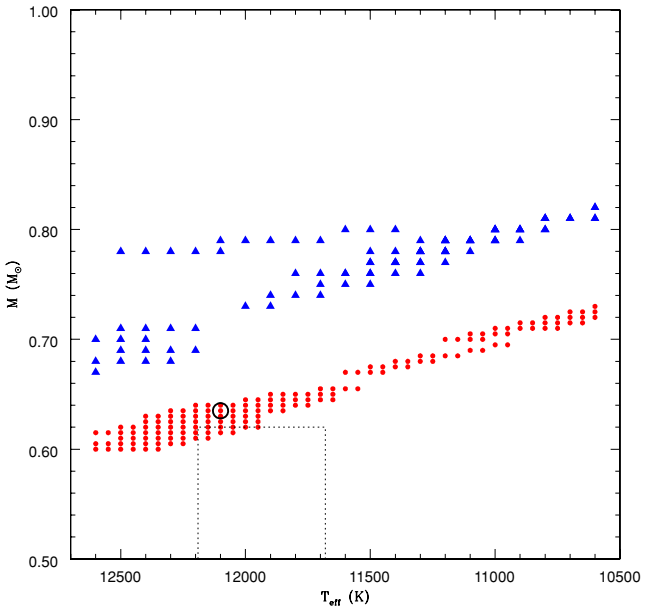


**Figure 1.** Results from comparison between the pulsation modes of the star R 548 to the models. The (red) circles are the solutions for $M_{\rm He} = 10^{-2}\,M_*$ and the (blue) triangles for $M_{\rm He} = 10^{-2.5}\,M_*$. There are no solutions for thinner He mass layer. The fitting was performed with the high-amplitude modes as $\ell = 1$ and the small amplitudes either $\ell = 1$ or 2. The dotted line box limits the region of the independent temperature and mass determinations ($\pm 1\sigma$) listed in Table 2, and the open circle shows the location of the minimum in $S$ for the best family of seismological solutions.

R 548 has five detected modes, so we started our analysis with this star, testing if all modes could be $\ell = 1$. Due to the small resulting period spacing between the 318 and 334 s modes (∼16 s), only seismological solutions for high mass were found, which is not in agreement with the two independent spectroscopic determinations, as listed in Table 1. For a fixed $\ell$ value, period is proportional to the inverse of the mean density squared ($P \propto 1/\sqrt{\rho}$), the excited modes are closer, like is the case for the ∼1 $M_\odot$ BPM 37093 (see Paper I, section 3.5). Therefore, it is necessary to test the possibility that the small-amplitude modes, at 333.64, 318.07 and 187.28 s, could be $\ell = 2$ modes. The families of solutions are shown in Fig. 1, and the minima for each family are listed in Table 2. All solutions in the families have similar probabilities. Solution 1 (open circle), with $T_{\rm eff} = 12\,100$ K and $M = 0.635\,M_\odot$, is the closest to the spectroscopy determinations (dotted line box). Our seismological studies in Paper I of G117−B15A and G185−32 indicate that they have thin H layer ($M_{\rm H} = 10^{-7}\,M_*$), in contrast to a thicker layer ($M_{\rm H} = 10^{-4.5}\,M_*$) of the most probable solution for R 548. This is not surprising as R 548 has different excited modes than G117−B15A and G185−32, at ∼318 and 333 s, which are probably the result of a different H layer thickness. The modes excited to visible amplitudes are probably the ones with nodes close to the transition zones between layers.

The other two members of this group, G132−12 and WD J2153−0731, have only one mode detected up to now. With only one mode detected, there is only one information to be obtained from seismology. For stars with only one solution, we had to make extra assumptions, not necessarily valid, to get any result. We hope our assumptions are valid on average, but we are not trustworthy for individual stars. We tested only the two internal structures determined for the multiperiodic star in this group, including the ones with modes around 215 s in Paper I: He layer mass layer of $10^{-2}\,M_*$ and the H layer mass either $10^{-4.5}$ or $10^{-7}\,M_*$. We fit only $\ell = 1$ modes, because the observed amplitudes are similar to other stars in this group. Another argument to expect similar internal structure is the similarities in spectroscopic temperature and mass. The minima of the best families of seismological solutions are listed in Table 3.

G132−12 is a bright star ($V = 16.2$) and, therefore, its spectroscopic temperature and mass determinations are reliable, which can be used to select between the several seismological solutions with similar probability. The difference between our seismological solution and spectroscopy in $T_{\rm eff}$ and $M$ are 70 K and 0.06 $M_\odot$ for $M_{\rm H} = 10^{-4.5}\,M_*$, and 500 K and 0.1 $M_\odot$ for $M_{\rm H} = 10^{-7}\,M_*$, indicating that the thick H layer solution is more likely. For WD J2153−0731, both thin and thick H seismological solutions are within the external spectroscopic uncertainties.

Our conclusion is that if the main mode is around 212 s, the He mass layer is probably $10^{-2}\,M_*$ and the H mass layer is probably either $10^{-4.5}$ or $10^{-7}\,M_*$. The detection of other modes and/or reliable temperature and mass determinations can be used to choose the most likely solution. Our approach does not find unique solutions, in general, but we expect the average for all stars to provide representative value.

### 2.2 Main period ∼200 s

The stars with main period around 200 s are listed in Table 4. L 19–2 and WD J1338−0023 are more massive and hotter than the others, which have mean spectroscopic temperature and mass of $T_{\rm eff} = 11\,740 \pm 30$ K and $M = 0.62 \pm 0.01\,M_\odot$. The stars in this group are cooler than the ones with ∼212 s main mode, in disagreement with the observed relation between $\langle P \rangle$ and $T_{\rm eff}$ (Mukadam et al. 2006). L 19–2 and WD J1338−0023, on the other hand, have temperatures typical of blue edge stars, but are more massive. That is the reason why they are studied separately.

**Table 2.** Seismology of R 548.

| Symbol in plot 1 | $T_{\rm eff}$ (K) | $M$ ($M_\odot$) | $-\log M_{\rm H}$ | $-\log M_{\rm He}$ | $S$ (s) | Modes ($\ell$, $k$) |
|---|---|---|---|---|---|---|
| Circles (red) | **12 100** | **0.635** | **4.5** | **2** | 0.28 | 183.8(2,3), 212.9(1,1) 274.5(1,2), 316.7(1,3) 338.2(2,9) |
| Triangles (blue) | 11 100 | 0.79 | 5.5 | 2.5 | 0.48 | 181.7(2,3), 213.2(1,2) 273.9(1,3), 313.8(1,4) 338.8(1,5) |

*Notes*. Absolute minima for the various families of solutions in the seismological analysis for the star R 548. The closest value to the spectroscopic solutions is solution 1. The bold font indicates the most likely solution.

**Table 3.** Seismology for G132−12 and WD J2153−0731.

| Star | $T_{\rm eff}$ (K) | $M$ ($M_\odot$) | $-\log M_{\rm H}$ | $-\log M_{\rm He}$ | $S$ (s) | Modes ($\ell$, $k$) |
|---|---|---|---|---|---|---|
| G132−12 | **12 150** | **0.63** | **4.5** | **2** | 0.06 | **212.8(1,2)** |
| | 11 500 | 0.67 | 7 | 2 | 0.02 | 212.7(1,1) |
| WD J2153−0731 | 12 300 | 0.64 | 4.5 | 2 | 0.02 | 210.2(1,2) |
| | 12 100 | 0.645 | 7 | 2 | 0.01 | 210.2(1,1) |

*Notes*. Absolute minima in $S$ for the two possible families of solutions in the seismological analysis of the stars G132−12 and WD J2153−0731.

**Table 4.** ZZ Ceti stars with main mode $P \sim 200$ s.

| Star | Modes (s) | Amp (mma) | $T_{\rm eff}$ (K) | $M$ ($M_\odot$) | Reference |
|---|---|---|---|---|---|
| WD J1354+0108 | 198.3 | 6.0 | 11 700 ± 50 | 0.61 ± 0.01 | Mukadam et al. (2004) |
| | 322.9 | 1.9 | | | |
| | 291.6 | 2.2 | | | |
| | 173.3 | 1.1 | | | |
| | 127.8 | 1.5 | | | |
| WD J0818+3132 | 202.3 | 3.3 | 11 800 ± 80 | 0.65 ± 0.02 | Mullally et al. (2005) |
| | 253.3 | 2.9 | | | |
| WD J1345−0055 | 195.2 | 5.5 | 11 800 ± 60 | 0.63 ± 0.02 | Mukadam et al. (2004) |
| | 254.4 | 2.4 | | | |
| WD J0847+4510 | 201.0 | 7.3 | 11 680 ± 110 | 0.61 ± 0.04 | Mukadam et al. (2004) |
| WD J0756+2020 | 199.5 | 6.8 | 11 710 ± 110 | 0.61 ± 0.03 | Mullally et al. (2005) |
| L 19–2 | 192.6 | 6.5 | 12 100 ± 200 | 0.74 ± 0.03 | Bergeron et al. (1995) |
| | 350.1 | 1.1 | 12 150 ± 100 | 0.70 ± 0.10 | Koester & Allard (2000) |
| | 143.4 | 0.6 | | | |
| | 118.7 | 1.2 | | | |
| | 113.8 | 2.4 | | | |
| WD J1338−0023 | 196.9 | 4.3 | 11 970 ± 80 | 0.69 ± 0.02 | Castanheira (2007) |
| | 119.9 | 2.3 | | | |
| | 254.8 | 2.2 | | | |

Of the normal mass pulsators of this group, WD J1354+0108 has the most detected modes, five. The modes and their respective normalized uncertainties, determined from the weights we use in the fits, proportional to amplitude squared are 198.3 ± 0.03, 291.6 ± 0.25, 322.9 ± 0.34, 127.8 ± 0.54 and 173.3 ± 1 s. We start by trying to fit $\ell = 1$ modes, but like for R 548, due to the small period spacing, $\Delta\bar{P} \sim 28$ s, only high-mass ($M > 0.84\,M_\odot$) seismological solutions were found. This is not a very likely solution, because the star is bright, $g = 16.36$, and the two independent SDSS spectra, with $S/N_{\,g} = 43$ each, should provide reliable temperature and mass. Even assuming that the main mode at 198 s and the other two highest amplitude modes, at 322.9 and 291.6 s, are $\ell = 1$, there is no seismological solution consistent within 1000 K and $0.1\,M_\odot$ of the spectroscopic temperature and mass. We searched our model grid for models around $M \sim 0.6\,M_\odot$ and $T_{\rm eff} \sim 11\,500$ K, but an $\ell = 1$ mode at $\sim 200$ s was never present. Therefore, the observed 198 s should be an $\ell = 2$ mode.

As the mass determinations are probably not wrong by $0.1\,M_\odot$ (seven times the internal uncertainty!) for all five stars in this subgroup, we assumed that the $\sim 200$ s mode is $\ell = 2$. Another strong argument in this direction is that the observed amplitudes, listed in Table 4, are smaller than the amplitudes of the main modes for other stars with similar temperatures. For example, the main mode of G117−B15A has an amplitude of ∼20 mma. The amplitude in this subgroup is inconsistent with the observational relationship that $A \propto 1/T_{\rm eff}$ (Mukadam et al. 2006).

Due to geometrical cancellation, $\ell = 1$ modes have higher observed amplitude than $\ell = 2$ of same intrinsic amplitude. As all other excited modes in WD J1354+0108 have smaller amplitudes than the main mode at 198 s, they were unconstrained in the fits as $\ell = 1$ or 2 modes. The minimum of the only seismological solution compatible with the spectroscopic determination is the model with $T_{\rm eff} = 11\,500$ K, $M = 0.64\,M_\odot$, $M_{\rm He} = 10^{-2}\,M_*$ and a thin H layer at $M_{\rm H} = 10^{-8}\,M_*$ (see Table 5). Only the mode at 291.6 s fits $\ell = 1$ better, while all the others fit $\ell = 2$.

WD J0818+3132 and WD J1345−0055 have very similar excited periodicities, so their internal structure should also be similar, confirmed by the minimum in $S$ of the families of solutions we found, listed in Table 5.

There are two stars, WD J0847+4510 and WD J0756+2020, with only one detected mode in this group. For them, we searched for solutions only within the internal structures obtained for the other stars: $M_{\rm He} = 10^{-2}\,M_*$ and $M_{\rm H} = 10^{-8}$ or $10^{-5}\,M_*$, and $M_{\rm He} = 10^{-2.5}\,M_*$ and $M_{\rm H} = 10^{-5}\,M_*$. In Table 5, we list the seismological

**Table 5.** Seismology for ZZ Ceti stars with main mode $P \sim 200$ s.

| Star | $T_{\rm eff}$ (K) | $M$ ($M_\odot$) | $-\log M_{\rm H}$ | $-\log M_{\rm He}$ | $S$ (s) | Modes in model ($\ell$, $k$) |
|---|---|---|---|---|---|---|
| WD J1354+0108 | 11 500 | 0.64 | 8 | 2 | 0.18 | 127.2(2,1), 169.7(2,2) 198.3(2,3), 292.5(1,2) 324.0(2,7) |
| WD J0818+3132 | 11 400 | 0.65 | 5 | 2.5 | 0.20 | 202.4(2,3), 253.0(2,5) |
| WD J1345−0055 | 11 600 | 0.645 | 5 | 2 | 0.17 | 195.4(2,3),254.1(2,5) |
| WD J0847+4510 | 11 600 | 0.55 | 5 | 2.5 | 0.03 | 201.0(2,3) |
| WD J0756+2020 | 11 100 | 0.67 | 5 | 2.5 | 0.03 | 195.5(2,3) |
| L 19–2 | 12 100 | 0.75 | 4.5 | 2 | 0.29 | 117.4(1,1), 192.5(1,2) 112.7(2,1), 135.0(2,2) 358.2(2,12) |
| WD J1338−0023 | 11 800 | 0.74 | 4.5 | 2 | 0.18 | 120.1(1,1), 196.7(1,2) 256.9(2,7) |

*Notes*. Most probable of the possible families of solutions in the seismological analysis for the ZZ Ceti stars with main mode at ∼200 s.

solutions compatible with spectroscopy, with both $M_{\rm H} = 10^{-5}\, M_*$ and $M_{\rm He} = 10^{-2.5}\, M_*$.

L 19–2 and WD J1338−0023 were studied separately from the other stars in this group because they have higher mass than the average. The $\ell$ choice for L 19–2 modes is based on the triplet and doublet measurements of O'donoghue & Warner (1982). They detected triplets for the high-amplitude modes around 192, 119 and 113 s, while the other modes were doublets. We call attention for the fact that one of the components of the triplets at 119 and 113 s was not well determined. Therefore, we tested all the possibilities of $\ell = 1$ and 2 for these modes. We recall again that the $\ell$ choices have to be consistent with period spacing. Considering geometrical cancellation increases with $\ell$ and the fact that the 118.7 s mode probably does not have the same $\ell$ as the 113.8 s mode as that would require $\Delta P \simeq 5$ s, the highest amplitude mode, at 113.8 s, should be $\ell = 1$. On the other hand, the 119 s mode was detected for WD J1338−0023, leading us to try the $\ell = 1$ possibility as well. As discussed previously in this section, the mode at 192.6 s can be $\ell = 1$ for these stars, because both have high mass. The seismological solutions consistent with spectroscopy are listed in Table 5. Our results for an $\ell = 2$ mode around 113 s are consistent with the rotational splitting observed by O'donoghue & Warner (1982), which is different than the splitting for the triplets around 192 and 119 s.

Both models have similar internal structures and the modes have the same $\ell$ value. None of the L 19–2 $\ell = 2$ modes was observed for WD J1338−0023. It is possible that amplitudes are below the detection limit, if they are excited. Bradley (2001) also studied L 19–2 seismologically, but the only difference to our results is that he identified the ∼350 s mode as $\ell = 1$. His results are $M_{\rm H} = 10^{-4}\, M_*$, $M_{\rm He} = 10^{-2}\, M_*$ and a 20:80 C/O core.

The study of this group allowed for the first time the detection of $\ell = 2$ as main pulsation modes in non-crystallized ZZ Ceti stars.

### 2.3 Main period between ∼200 and ∼210 s

We decided to study these stars in a separated group because the set of excited periods is slightly different than the groups whose main modes are ∼210 and ∼200 s (see Table 6), but similar among themselves. Despite similar external temperatures, this fact might result in internal structures different than in the other groups (with main modes at $P \sim 200$ and ∼212 s).

We started testing if all modes were $\ell = 1$, but as we found no solution for LP 133−144, we allowed the low-amplitude modes to be $\ell = 2$. In Table 7, we list the minima in $S$ for the families of solutions.

HS 0951+1312 spectroscopic mass determination is not accurate, because data were obtained with a low-resolution objective prism (Homeier & Koester 2001). The most probable seismological solution is hotter ($T_{\rm eff} = 12\,400$ K) and less massive ($M = 0.655\, M_\odot$) than for LP 133−144, in agreement with $\langle P \rangle = 243.9$ s that places this star near the blue edge of the ZZ Ceti instability strip.

The other star of this group, G238−53, has only one detected mode at 206 s. We searched only within the families of solutions of models with the same internal structure as determined for the other members of this group: $M_{\rm He} = 10^{-2}\, M_*$ and $M_{\rm H} = 10^{-5}$ or $10^{-7}\, M_*$, but we did not find solution consistent with the spectroscopic determination. As temperature and mass determinations are reliable, we looked for solutions within the uncertainties of these values, which are listed in Table 7. The detection of more modes, if present, is fundamental to better constrain the structure of G238−53.

### 2.4 Main period at ∼250 s

There are only two stars in this group, EC 11507−1519 and WD J0939+5609, with one or two detected modes, which restricts our investigation about these stars. In addition, WD J0939+5609 is faint, $g = 18.70$, therefore the $S/N_g = 15$ SDSS spectrum does not provide accurate temperature nor mass (see Table 8).

Starting with EC 11507−1519, we test if both known modes can be $\ell = 1$. The problem is the same as when the main mode is ∼200 s: only high-mass and/or high-temperature models have this mode, inconsistent with the spectroscopic determination. Therefore, the 191.7 s mode was fit by $\ell = 2$. Because there is no seismological solution if the main mode was $\ell = 1$, both modes were fit to $\ell = 2$, and the minimum in $S$ of the family of solutions consistent with spectroscopy is $T_{\rm eff} = 12\,000$ K and $M = 0.605\, M_\odot$ (see Table 9).

**Table 6.** ZZ Ceti stars with main mode between 200 and 210 s.

| Star | Modes (s) | Amp (mma) | $T_{\rm eff}$ (K) | $M$ ($M_\odot$) | Reference |
|---|---|---|---|---|---|
| LP 133−144 | 209.2 | 10 | 11 800 ± 200 | 0.54 ± 0.02 | Bergeron et al. (2004) |
| | 305.7 | 5.3 | | | |
| | 327.3 | 4.0 | | | |
| HS 0951+1312 | 208.0 | 9.3 | 11 000 ± 500 | 0.4 ± 0.2 | Homeier & Koester (2001) |
| | 281.6 | 8.8 | | | |
| | 258.6 | 3.6 | | | |
| G238−53 | 206 | 9 | 11 890 ± 200 | 0.55 ± 0.02 | Bergeron et al. (2004) |
| | | | 11 820 ± 50 | 0.62 ± 0.01 | Kepler et al. (2007) |

**Table 7.** Seismology for LP 133−144, HS 0951+1312 and G238−53.

| Star | $T_{\rm eff}$ (K) | $M$ ($M_\odot$) | $-\log M_{\rm H}$ | $-\log M_{\rm He}$ | $S$ (s) | Modes ($\ell$, $k$) |
|---|---|---|---|---|---|---|
| LP 133−144 | 11 700 | 0.52 | 5 | 2 | 1.00 | 209.9(1,2), 303.9(2,7) |
| | | | | | | 331.2(2,8) |
| HS 0951+1312 | 11 900 | 0.69 | 7 | 2 | 2.57 | 205.7(1,1), 246.0(1,2) |
| | | | | | | 283.5(1,3) |
| | **12 400** | **0.655** | **5** | **2** | 0.40 | 207.7(1,1), 281.7(1,2) |
| | | | | | | 261.3(2,6) |
| G238−53 | 11 400 | 0.525 | 7 | 2 | 0.03 | 205.69(1,1) |
| | 12 200 | 0.57 | 5.5 | 2 | 0.09 | 206.09(1,1) |
| | 11 400 | 0.57 | 5.5 | 2.5 | 0.04 | 206.96(1,1) |
| | 11 800 | 0.64 | 6 | 3 | 0.15 | 206.15(1,1) |

*Notes*. Absolute minima in $S$ for two possible families of solutions in the seismological analysis of the stars LP 133−144, HS 0951+1312 and G238−53.

**Table 8.** ZZ Ceti stars with main mode $P \sim 250$ s.

| Star | Modes (s) | Amp (mma) | $T_{\rm eff}$ (K) | $M$ ($M_\odot$) | Reference |
|---|---|---|---|---|---|
| EC 11507−1519 | 249.6 | 7.7 | 12 030 ± 200 | 0.60 ± 0.03 | Gianninas et al. (2006) |
| | 191.7 | 3.59 | | | |
| WD J0939+5609 | 249.9 | 7.2 | 11 790 ± 60 | 0.75 ± 0.05 | Eisenstein et al. (2006) |

**Table 9.** Seismology for EC 11507−1519 and WD J0939+5609.

| Star | $T_{\rm eff}$ (K) | $M$ ($M_\odot$) | $-\log M_{\rm H}$ | $-\log M_{\rm He}$ | $S$ (s) | Modes ($\ell$, $k$) |
|---|---|---|---|---|---|---|
| EC 11507−1519 | 12 000 | 0.605 | 4.5 | 2 | 0.11 | 191.5(2,3), 249.7(2,5) |
| WD J0939+5609 | **11 500** | **0.77** | **4.5** | **2** | 0.07 | 250.0(2,7) |
| | 12 350 | 0.58 | 4.5 | 2 | 0.005 | 249.9(2,5) |
| | 11 400 | 0.705 | 4.5 | 2 | 0.011 | 249.9(2,6) |

*Notes*. Absolute minima in $S$ for the two possible families of solutions from the seismological analysis for the stars EC 11507−1519 and WD J0939+5609, using only the same internal solution as for the first one.

Assuming that the spectroscopic masses of these stars are within $0.1\,M_\odot$ of the real solution, the presence of the 191.7 s mode indicates a smaller mass for EC 11507−1519. On the other hand, if these stars have similar structures, the 192 s mode could be below the actual detection limits for WD J0939+5609. For the same internal structure, i.e. $M_{\rm H} = 10^{-4.5}\,M_*$ and $M_{\rm He} = 10^{-2}\,M_*$, we test only two mass values: $0.6\,M_\odot$, the mean mass value for white dwarfs with H-dominated atmospheres (Kepler et al. 2007), and around $0.75\,M_\odot$, near the spectroscopic value. The possible families of solutions for $\ell = 2$ are listed in Table 9.

### 2.5 Main mode ∼260 s

The 13 stars with main excited mode around 260 s are listed in Table 10. The two stars with most detected modes in this group are WD J0913+4036 and WD J1007+5245, with four periodicities each. For WD J1007+5245, the periodicity at 152.8 s is at the linear combination frequency of two modes ($f_1$ and $f_2$) of WD J1007+5245, even though it has amplitude of the same order as the parent modes. In a first moment, we did not consider this periodicity as an independent mode. For WD J0913+4036, a mode at 203.9 s

**Table 10.** ZZ Ceti stars with main mode at $P \sim 260$ s.

| Star | Modes (s) | Amp (mma) | $T_{\rm eff}$ (K) | $M$ ($M_\odot$) | Reference |
|---|---|---|---|---|---|
| WD J0913+4036 | 260.3 | 16.5 | 11 680 ± 80 | 0.54 ± 0.02 | Mullally et al. (2005) |
| | 320.5 | 14.7 | | | |
| | 288.7 | 12.4 | | | |
| | 203.9 | 3.8 | | | |
| WD J1007+5245 | 258.8 ($f_1$) | 11.0 | 11 430 ± 130 | 0.66 ± 0.05 | Mullally et al. (2005) |
| | 323.1 ($f_2$) | 10.4 | | | |
| | 290.1 ($f_3$) | 7.7 | | | |
| | 152.8 ($f_2 + f_3$) | 5.8 | | | |
| KUV 11370+4222 | 257.2 | 5.3 | 11 890 ± 200 | 0.64 ± 0.03 | Bergeron et al.2004 |
| | 292.2 | 2.5 | | | |
| | 462.9 | 3.2 | | | |
| WD J1125+0345 | 265.5 | 7.2 | 11 600 ± 120 | 0.60 ± 0.04 | Mukadam et al. (2004) |
| | 208.6 | 2.8 | | | |
| WD J0958+0130 | 264.4 | 4.7 | 11 680 ± 60 | 0.60 ± 0.02 | Mukadam et al. (2004) |
| | 203.7 | 2.5 | | | |
| WD J2214−0025 | 255.2 | 13.1 | 11 440 ± 80 | 0.82 ± 0.03 | Mullally et al. (2005) |
| | 195.2 | 6.1 | | | |
| GD 385 | 256 | 11.2 | 11 710 ± 200 | 0.63 ± 0.03 | Bergeron et al. (2004) |
| | 128.1 | 3.7 | | | |
| WD J0018+0031 | 257.3 | 6.0 | 11 700 ± 80 | 0.57 ± 0.02 | Mullally et al. (2005) |
| | 149.9 | 3.7 | | | |
| WD J0853+0005 | 264.4 | 4.0 | 11 750 ± 110 | 0.68 ± 0.04 | Castanheira (2007) |
| WD J1218+0042 | 258 | 16 | 11 123 ± 93 | 0.71 ± 0.04 | Kepler et al. (2005b) |
| WD J1136−0137 | 260.8 | 3.1 | 11 710 ± 700 | 0.59 ± 0.02 | Castanheira (2007) |
| MCT 2148−2911 | 260.8 | 12.6 | 11 740 ± 200 | 0.51 ± 0.02 | Gianninas et al. (2005) |
| WD J1533−0206 | 259.2 | 4.8 | 11 350 ± 40 | 0.73 ± 0.02 | Castanheira et al. (2006) |

is excited, which should be $\ell = 2$, based on its low mass and the same arguments discussed in Section 2.2. The other excited modes are very similar in both stars, not only the periods, but also the amplitudes. We expect similar structures for WD J0913+4036 and WD J1007+5245. The WMP, $\langle P \rangle$, is 286 and 275 s, respectively, which provides $T_{\rm eff}$ around 11 900 K (Mukadam et al. 2006) for both stars. The period spacing between the three main modes is $\Delta \bar{P} \sim 30$ and ∼32 s, respectively, implying that the masses should also be similar, within the spectroscopic external uncertainties. In Table 11, the minima of the best families of seismological solutions for these two stars are given, confirming that they have very similar structures.

Even though the seismological mass for WD J1007+5245 is 0.1 $M_\odot$ different than the spectroscopic value, this star is rather faint ($g = 18.87$), which means that the S/N $_g \simeq 13.7$ SDSS spectrum provides uncertain mass.

KUV 11370+4222 has three excited modes known, but instead of a 320 s mode, the 462.9 s mode is excited. The minima of the possible solutions, with structure different than the one determined for the other two stars of this group, are listed in Table 11; the second solution is much more probable than the first one ($S$ is five times smaller).

There is a subgroup of stars with two modes, where the second is ∼200 s. WD J1125+0345 and WD J0958+0130 show similar modes and spectroscopic temperature and mass. The mode at ∼200 s should be $\ell = 2$, not only because the temperatures are not typical of the blue edge, but also because $\Delta P \sim 60$ s, implying very low masses, if they were $\ell = 1$ and consecutive $k$. The minima of the best families of solutions are listed in Table 11.

WD J2214−0025 is very similar to WD J1125+0345 and WD J0958+0138, but its main mode is 10 s shorter than the observed in other stars and its spectroscopic mass is 0.82 $M_\odot$, from a reliable determination ($g = 17.91$, S/N$_g \simeq 22.7$). An $\ell = 1$ mode could only be present for high-mass ($M > 0.75\,M_\odot$) stars at the blue edge ($T_{\rm eff} \sim 12\,200$ K). Even though the high mass requirement is satisfied, its temperature places the star in the middle of the instability strip. Therefore, the 195.2 s mode should be $\ell = 2$. On the other hand, there is yet another possibility that the H layer mass is much thinner. The seismological solutions consistent with spectroscopy are listed in Table 11.

Besides the main mode, WD J0018+0031 and GD 385 pulsate with small-amplitude modes at 149.9 and 128.1 s, respectively. The 128.1 s mode has the same frequency as the harmonic of the main mode for GD 385, but this was the only period excited in some runs, indicating that this is probably another real mode. The seismological solutions for these stars are listed in Table 11.

There are five stars with only one excited mode, for which we tested the possible solutions derived from the other stars of this group with more modes. The minima in $S$ of the families of solutions are also listed in Table 11.

**Table 11.** Seismology for ZZ Ceti stars with main mode $P \sim 260$ s.

| Star | $T_{\rm eff}$ (K) | $M$ ($M_\odot$) | $-\log M_{\rm H}$ | $-\log M_{\rm He}$ | $S$ (s) | Modes ($\ell$, $k$) |
|---|---|---|---|---|---|---|
| WD J0913+4036 | 11 700 | 0.53 | 6.5 | 3.5 | 1.89 | 206.0(2,3), 258.5(1,1) 292.4(1,2), 320.8(1,3) |
| WD J1007+5245 | 11 600 | 0.53 | 6.5 | 3.5 | 1.16 | 150.4(2,1), 259.5(1,1) 293.1(1,2), 323.6(1,3) |
| KUV 11370+4222 | 12 000 | 0.685 | 4.5 | 2 | 1.46 | 256.7(1,3), 298.9(1,3) 461.9(1,8) |
| | **11 900** | **0.66** | **7** | **2** | 0.43 | 257.5(1,2), 290.8(1,3) 463.4(1,6) |
| WD J1125+0345 | 11 900 | 0.58 | 6.5 | 3 | 0.30 | 209.5(2,3), 265.7(1,2) |
| | **11 600** | **0.66** | **7** | **3.5** | 0.30 | 208.6(2,3), 265.2(1,2) |
| WD J0958+0130 | **11 500** | **0.58** | **6.5** | **2.5** | 1.65 | 198.2(2,3), 265.2 (1,2) |
| | 12 200 | 0.58 | 6.5 | 3 | 0.71 | 206.2(2,3), 264.2(1,2) |
| WD J2214−0025 | 12 000 | 0.84 | 9.5 | 2.5 | 0.05 | 195.0(1,1), 225.2(1,2) |
| | **11 500** | **0.775** | **8.5** | **2** | 0.02 | 195.3(1,1), 255.2(2,6) |
| | 11 300 | 0.75 | 8.5 | 3.5 | 0.12 | 195.7(2,3), 255.3(2,5) |
| WD J0018+0031 | **11 600** | **0.63** | **4** | **2** | 0.32 | 149.1(2,2), 257.4(1,3) |
| | 11 400 | 0.60 | 6.5 | 2.5 | 0.46 | 148.9(2,2), 257.5(1,2) |
| GD 385 | **11 700** | **0.595** | **6.5** | **2** | 0.12 | 129.2(2,1), 256.0(1,2) |
| | 11 800 | 0.67 | 7 | 2.5 | 0.17 | 128.5(2,1), 255.8(1,2) |
| WD J0853+0005 | 12 200 | 0.66 | 4.5 | 2 | 0.06 | 264.5(1,2) |
| | 11 700 | 0.60 | 6.5 | 3.5 | 0.11 | 264.5(1,2) |
| WD J1136−0137 | 11 950 | 0.58 | 6.5 | 2 | 0.05 | 260.9(1,2) |
| WD J1218+0042 | 11 000 | 0.70 | 4.5 | 2 | 0.02 | 258.0(1,3) |
| WD J1533−0206 | 11 400 | 0.755 | 4 | 2 | 0.06 | 259.0(1,4) |
| | 11 100 | 0.695 | 4.5 | 2 | 0.03 | 259.1(1,3) |
| MCT 2148−2911 | 11 900 | 0.51 | 6.5 | 3.5 | 0.01 | 260.8(1,1) |

*Notes*. Absolute minima in $S$ for the families of solutions in the seismological analysis for the stars with main mode ∼260 s.

### 2.6 Main period ∼270 s

The stars with main period around 270 s (Table 12) are located in the middle of the ZZ Ceti instability strip.

The star with most observed modes in the group is GD 66. On top of the four excited modes, GD 66 has seven other periodicities detected, harmonics and linear combinations. This star has been constantly observed for precise measurements of phase shifts by Mullally et al. (2008), who measured $\dot{P} \sim 100$ times faster than the cooling theory predictions, and propose that this is due to a planetary companion, still to be confirmed. Starting our seismological analysis with this star, if we assume that all modes were $\ell = 1$, the mass should be at least $0.8\,M_\odot$, in contradiction with the spectroscopic determinations. Another solution is for a temperature hotter than the blue edge, if only the smallest amplitude mode, 256.0 s, is $\ell = 2$. Once again, as in Section 2.2, the normal spectroscopic mass indicates that the 197.4 s mode is also $\ell = 2$. One problem is that we are claiming to have detected several linear combinations involving $\ell = 1$ and 2 modes. Even with no selection rule to prevent different $\ell$ to produce linear combinations, they are less likely than combinations involving same $\ell$ degree modes. Among all families of seismological solutions, the closest to the spectroscopic determinations is at $T_{\rm eff} = 12\,400$ K and $M = 0.64\,M_\odot$, with relatively thin H and He layers, $M_{\rm H} = 10^{-7}\,M_*$ and $M_{\rm He} = 10^{-3.5}\,M_*$, listed in Table 13. None of the other minima has temperature lower than this value, slightly hotter than the spectroscopic blue edge.

WD J1015+0306 has the same excited periods as GD 66, although it does not show the mode near 300 s. The seismological solution we found has very similar structure as GD 66, as shown in Table 13.

WD J1002+5818 looks like a complementary star in terms of detected modes to WD J1015+0306, in relation to GD 66. There is one solution with very similar structure, with $T_{\rm eff} = 12\,300$ K, $M = 0.53\,M_\odot$, $M_{\rm H} = 10^{-7.5}\,M_*$ and $M_{\rm He} = 10^{-3.5}\,M_*$, also listed in Table 13.

WD J1724+5835 differs from HE 0031−5525 in having one extra detected mode at 189.2 s. These two stars have low masses and are located in the middle of the instability strip. Because of their masses, a large period spacing ($\Delta P \sim 55$ s) is expected, therefore, the ∼280 and ∼ 330 s modes should have the same $\ell$ degree and consecutive $k$s. The minima of seismological families of solutions are listed in Table 13. This group has relatively thin H layers, $10^{-6.5} \leq M_{\rm H}/M_* \leq 10^{-7.5}$.

WD J0959+0238 has the longest main amplitude excited mode of this group, around 283 s. As for the other stars in the 270 s main mode group, there is no seismological solution in agreement with

**Table 12.** Main mode $P \sim 270$ s.

| Star | Modes (s) | Amp (mma) | $T_{\rm eff}$ (K) | $M$ ($M_\odot$) | Reference |
|---|---|---|---|---|---|
| GD 66 | 271.68 ($f_1$) | 16.97 | 11 980 ± 200 | 0.64 ± 0.03 | Bergeron et al. (2004) |
| | 302.78 ($f_2$) | 11.43 | | | |
| | 255.98 ($f_3$) | 3.81 | | | |
| | 197.39 ($f_4$) | 5.44 | | | |
| | 522.14 ($f_1 + f_2 - f_4$) | 2.26 | | | |
| | 143.21 ($f_1 + f_2$) | 2.72 | | | |
| | 135.88 ($2 \times f_1$) | 1.82 | | | |
| | 131.79 ($f_1 + f_3$) | 1.43 | | | |
| | 114.30 ($f_1 + f_4$) | 1.65 | | | |
| | 567.85 ($f_4 - f_2$) | 1.52 | | | |
| | 119.60 ($f_2 + f_4$) | 1.33 | | | |
| WD J1015+0306 | 270.0 | 8.4 | 11 580 ± 30 | 0.70 ± 0.01 | Mukadam et al. (2004) |
| | 255.7 | 7.3 | | | |
| | 194.7 | 5.8 | | | |
| WD J1002+5818 | 268.2 | 6.8 | 11 710 ± 130 | 0.57 ± 0.03 | Mullally et al. (2005) |
| | 304.6 | 5.3 | | | |
| HE 0031−5525 | 276.9 | 4.6 | 11 480 ± 30 | 0.44 ± 0.01 | Castanheira et al. (2006) |
| | 330.8 | 2.5 | | | |
| WD J1724+5835 | 279.5 | 8.3 | 11 540 ± 80 | 0.55 ± 0.02 | Mukadam et al. (2004) |
| | 337.9 | 5.9 | | | |
| | 189.2 | 3.2 | | | |
| WD J0959+0238 | 283.9 | 12.3 | 11 830 ± 110 | 0.64 ± 0.04 | Eisenstein et al. (2006) |
| | 254.0 | 6.6 | | | |
| | 194.0 | 5.8 | | | |

**Table 13.** Seismology for stars with main mode around 270 s.

| Star | $T_{\rm eff}$ (K) | $M$ ($M_\odot$) | $-\log M_{\rm H}$ | $-\log M_{\rm He}$ | $S$ (s) | Modes ($\ell$, $k$) |
|---|---|---|---|---|---|---|
| GD 66 | 12 400 | 0.64 | 7 | 3.5 | 2.88 | 199.3(2,3), 257.1(2,5) 268.7(1,2), 305.1(1,3) |
| WD J1015+0306 | 12 100 | 0.71 | 7.5 | 3.5 | 7.18 | 195.2(2,3), 254.5(2,5) 270.3(1,2) |
| WD J1002+5818 | 12 300 | 0.53 | 7.5 | 3.5 | 1.13 | 268.0(1,2), 304.8(1,3) |
| HE 0031−5525 | 11 000 | 0.555 | 6.5 | 2 | 0.21 | 277.1 (1,2), 330.3 (1,3) |
| | 12 100 | 0.55 | 6.5 | 2.5 | 1.82 | 275.6 (1,2), 335.4 (1,3) |
| WD J1724+5835 | 10 600 | 0.555 | 6.5 | 2 | 1.14 | 195.3 (2,3), 279.5 (1,2) 336.1 (1,3) |
| | | | 6.5 | 2.5 | 1.98 | 202.6 (2,3), 280.4 (1,2) 336.9 (1,3) |
| WD J0959+0238 | 11 700 | 0.68 | 7.5 | 3 | 0.96 | 190.5 (2,3), 255.7 (2,5) 283.4 (1,2) |

*Notes*. Absolute minima in $S$ in the possible families of solution in the seismological analysis.

the spectroscopic determination if both 194 and 254 s are fixed to be $\ell = 1$; they are probably $\ell = 2$. The seismological solution is listed in Table 13.

### 2.7 Main period ∼300 s

As the stars cool, the modes increase in period, consistent with the d$P$/d$t$ measured for G117−B15A (Kepler et al. 2005a). The convective zone gets deeper, and more modes are available to be excited theoretically. Stars with longer periods are observed to pulsate in more frequencies, which provides more independent measurements, but more complicated to find similarities. Table 14 shows all the eight stars that belong to this group.

WD J0111+0018 has a main mode around 293 s and the lower amplitude modes are shorter than this. If our understanding about pulsations in ZZ Ceti stars is correct, the stars of this group are on average cooler than the ones in the previous groups, but there is no reason to expect their internal structure to be different. Excluding linear combinations and harmonics, WD J0111+0118 has almost the same modes detected for KUV 11370+4222 (Section 2.5), except for the 462.9 s mode. The seismological solution is $T_{\rm eff} = 11\,450$ K, $M = 0.67\,M_\odot$, $M_{\rm H} = 10^{-7}\,M_*$ and $M_{\rm He} = 10^{-2}\,M_*$ (Table 15), similar to that derived for KUV 11370+4222 (see

**Table 14.** Main mode $P \sim 300$ s.

| Star | Modes (s) | Amp (mma) | $T_{\rm eff}$ (K) | $M$ ($M_\odot$) | Reference |
|---|---|---|---|---|---|
| WD J0111+0018 | 292.97 ($f_1$) | 22.13 | 11 510 ± 100 | 0.77 ± 0.04 | Mukadam et al. (2004) |
| | 255.50 ($f_2$) | 12.95 | | | |
| | 136.54 ($f_1 + f_2$) | 7.49 | | | |
| | 146.49 ($2 \times f_1$) | 5.37 | | | |
| GD 244 | 307.1 | 20.2 | 11 680 ± 200 | 0.66 ± 0.03 | Fontaine et al. (2003) |
| | 256.6 | 12.3 | | | |
| | 203.0 | 4.0 | | | |
| WD J2128−0007 | 302.2 | 17.1 | 11 440 ± 100 | 0.79 ± 0.05 | Castanheira et al. (2006) |
| | 274.9 | 11.0 | | | |
| | 289.0 | 9.7 | | | |
| WD J2350−0054 | 304.3 | 17.0 | 10 350 ± 60 | 0.80 ± 0.04 | Mukadam et al. (2004) |
| | 391.1 | 7.5 | | | |
| | 273.3 | 6.2 | | | |
| WD J0917+0926 | 288.5 | 15.05 | 11 340 ± 70 | 0.70 ± 0.04 | Kepler et al. (2005b) |
| | 260.0 | 9.4 | | | |
| | 211.5 | 9.2 | | | |
| WD J0214−0823 | 297.06 ($f_1$) | 15.70 | 11 570 ± 90 | 0.57 ± 0.02 | Mukadam et al. (2004) |
| | 263.21 ($f_2$) | 6.97 | | | |
| | 347.30 ($f_3$) | 6.58 | | | |
| | 174.05 ($2 \times f_3$) | 1.81 | | | |
| | 149.00 ($2 \times f_1$) | 2.07 | | | |
| HS 1249+0426 | 288.9 | 7.55 | 11 770 ± 200 | 0.57 ± 0.02 | Voss et al. (2006) |
| WD J0842+3707 | 309.3 | 17.9 | 11 720 ± 170 | 0.48 ± 0.03 | Mukadam et al. (2004) |

**Table 15.** Seismology for ZZ Ceti stars with main mode 300 s.

| Star | $T_{\rm eff}$ (K) | $M$ ($M_\odot$) | $-\log M_{\rm H}$ | $-\log M_{\rm He}$ | $S$ (s) | Modes ($\ell$, $k$) |
|---|---|---|---|---|---|---|
| WD J0111+0118 | 11 450 | 0.67 | 7 | 2 | 0.33 | 255.8(1,2), 293(1,3) |
| GD 244 | 12 200 | 0.68 | 7 | 3.5 | 0.28 | 199.4(2,3), 256.6(2,5) 307.4(1,3) |
| WD J2128−0007 | 12 100 | 0.83 | 8.5 | 3.5 | 0.64 | 275.7(1,2), 288.7(1,3) 301.6(1,4) |
| WD J2350−0054 | 10 600 | 0.74 | 8 | 2 | 0.86 | 279.9(1,2), 304.4(1,3) 391.4(1,5) |
| | 11 600 | 0.84 | 8.5 | 3.5 | 0.39 | 274.9(1,2), 304.5(1,3) 392.3(1,5) |
| WD J0917+0926 | 12 100 | 0.67 | 7.5 | 3.5 | 1.59 | 215.0(2,4), 260.4(2,5) 287.3(1,2) |
| WD J0214−0823 | 11 200 | 0.52 | 6.5 | 3 | 1.52 | 256.6(1,1), 296.9(1,2) 352.22(1,3) |
| HS 1249+0426 | 11 800 | 0.55 | 4 | 2 | 0.01 | 288.89(1,2) |
| | 12 000 | 0.59 | 7 | 2.5 | 0.004 | 288.90(1,2) |
| | 11 800 | 0.53 | 6.5 | 3 | 0.02 | 288.92(1,2) |
| | 11 500 | 0.6 | 7 | 3 | 0.05 | 291.01(1,2) |
| WD J0842+3707 | 11 600 | 0.56 | 7 | 3.5 | 0.29 | 309.59(1,2) |

*Notes*. Absolute minima in $S$ for two possible families of solutions in the seismological analysis for the ZZ Ceti stars with main mode 300 s.

Table 11), but a little cooler, as expected. Because it is a faint star, $g = 18.8$, the spectroscopic mass is uncertain. The period spacing is ∼40 s, corresponding to a mass smaller than the spectroscopic mass.

As argued in Section 2.2, the 203.0 s mode detected for GD 244 is probably an $\ell = 2$. This star is very similar to GD 66, but the main mode is longer, indicating that this star should be a little cooler, like in the previous case. The seismological solution is $T_{\rm eff} = 12\,200$ K,

$M = 0.68\,M_\odot$, and thin H and He layers, $M_H = 10^{-7}\,M_*$, and $M_{He} = 10^{-3.5}\,M_*$, listed in Table 15, with the same internal structure as GD 66 and the same observed modes of both stars have the same $\ell$ and $k$. For the first time, we have detected evolutionary sequences for those two pairs of stars and consistent with the observational determination by Giovannini et al. (1998) that the instability strip moves to higher $T_{eff}$ for higher masses.

The excited modes of WD J2128−0007 and WD J2350−0054 are very similar, but because of its smaller $\langle P \rangle$ and similar masses, WD J2128−0007 should be slightly hotter than WD J2350−0054. Because of the high masses and similar amplitudes among the observed modes, all of them could be fit to $\ell = 1$. WD J2128−0007 is 1 mag brighter than WD J0111+0118, therefore, its spectroscopic mass should not be wrong by $0.1\,M_\odot$, i.e. this star has a mass above the average of the white dwarf mass distribution. However, if all modes are $\ell = 1$, the seismological temperature is 600 K hotter than the spectroscopy value. As first determined by Giovannini et al. (1998), there is a small dependence in mass in the position of the edges of the ZZ Ceti instability strip. For example, G226−29 is the hottest ZZ Ceti and has a mass around $0.8\,M_\odot$. According to our seismological analysis for this star, the most probable temperature is 12 400 K, what defines the blue edge for this mass (see discussion in Paper I). Our seismological temperature at 12 100 K is consistent with the observed periods and the position of WD J2128−0007 towards the middle of the instability strip.

WD J2350−0054 deserves special attention, because its spectroscopic temperature ($T_{eff} \sim 10\,350$ K, from two independent SDSS spectra with S/N = 16.5 and 18.7) places this star way outside the instability strip. According to its periodicities, this star should be in the middle of the strip. The most surprising is that there is one seismological solution for low temperature, similar to the spectroscopic determination, as shown in Table 15. Our model grid uses the adiabatic approximation, i.e. we do not calculate which modes are excited, but compute all the modes compatible with a particular structure. Searching for solutions with the same structure as determined for WD J2128−0007, we found that the seismological temperature for WD J2350−0054 is consistent with the observed periods (see Table 15).

No seismological solution was found for WD J0917+0926, if all modes were $\ell = 1$. However, the smaller observed amplitudes for 260.0 and 211.5 s modes are consistent with $\ell = 2$, when compared to the amplitude of the 288.5 s mode. The seismological solution we found (see Table 15) is hotter than the spectroscopic value, but it is consistent with the expected temperature from its $\langle P \rangle$.

The star WD J0214−0823 has, in fact, low seismological mass and all modes fit $\ell = 1$, as shown in Table 15.

HS 1249+0426 has only one detected mode, but its temperature and mass are well determined. Therefore, we looked only for solutions consistent with this determination, listed in Table 15.

Another star with only one detected mode is WD J0842+3707, which is closer to the main mode of GD 244. We searched only for solutions compatible with the structure found for GD 244. If its structure is similar to the one determined to GD 244 (see Table 15), the uncertainty in spectroscopic mass is twice the internal value.

### 2.8 Main period between 300 and 500 s

Tables 16, 18 and 20 show the 14 stars that belong to this group. As mentioned in Section 2.7, similarities among the stars are more difficult to find. That is why we separated them in subgroups.

In Table 16, we list the stars of this group, with averages in spectroscopic temperature and mass of 11 480 ± 130 K and $0.63 \pm 0.03\,M_\odot$. In the upper panel of Fig. 2, we plot all detected periods and amplitudes for these stars and in the lower panel, the computed mean values with bins from −5 to +5 s difference of the high-amplitude modes (listed in Table 17).

We included in this subgroup the stars WD J0949−0000 and HE 0344+1207, because they have similar observed periods and amplitudes, despite their spectroscopic temperature and/or mass being a few $\sigma$ different from the mean values calculated for the other stars. WD J0949−0000 is a faint star, $g = 18.8$, therefore, the spectroscopic determinations are uncertain (two spectra with $S/N_g = 9$ and 12). Even though HE 0344+1207 is a bright star, $B = 15.8$, temperature and mass were determined from photometry alone, as no spectra is available. We compared the average modes to our model grid and found that the only seismological solution compatible with the average temperature and mass and all modes $\ell = 1$ is the model with $T_{eff} = 11\,400$ K, $M = 0.69\,M_\odot$, $M_H = 10^{-4}\,M_*$ and $M_{He} = 10^{-2}\,M_*$. In Table 17, we list the modes present in the model.

If WD J0949−0000 also belongs to this subgroup, the difference from the seismological results and the SDSS spectroscopic temperature is 220 K and $0.06\,M_\odot$ in mass. Temperature and mass were determined by low-S/N spectrum. For faint stars with many detected modes, like this one, we are able to estimate the external uncertainties to the spectroscopic measurements. In the case of HE 0344+1207, the difference in mass is $0.09\,M_\odot$, indicating a more realistic value for the mass uncertainty to the photometric determination.

G207−9 and WD J0815+4437, listed in Table 18, were studied together because of their similar excited modes. As WD J0815+4437 has an apparent magnitude of $g = 19.3$, its mass is not well determined. On the other hand, G207−9 is bright, $V = 14.6$ and has two independent determinations of $T_{eff}$ and $M$. In Fig. 3, we plot the detected modes (upper panel) for these two stars, and mean values (lower panel), which are listed in Table 19.

The pulsation spectra of these two stars show different observed amplitudes. It is possible that we are observing the stars from different viewing angles. Despite this, we observe an amplitude modulation in both stars, which we used to estimate the amplitudes of missing modes to calculate average amplitudes. It is very important that the energy carried by each mode is conserved when we average out the amplitudes of modes detected in distinct stars.

In Fig. 4, we show the two seismological solutions. The (red) circles come from the best model for G207−9, which agrees with the spectroscopic determinations. Surprisingly, there is yet a low-mass solution at $0.53\,M_\odot$, with different $M_H$ and $M_{He}$, similar to the spectroscopic value for WD J0815+4437, which is also consistent with our seismological study.

The stars listed in Table 20 have only one or two detected modes, and their spectroscopic determinations are not similar to the others stars of this group. There should be other excited modes in these stars, below the actual detection limits, and follow-up observations are crucial to study these stars. In the red part of the instability strip, it is more complex to break the degeneracy of the solutions, because the higher $k$ modes converge to the asymptotic spacing, losing their individual signature of the stellar structure. This behaviour is the opposite of what happens for the stars in the blue part, which have lower $k$ modes, very sensitive to small variations of the stellar structure.

**Table 16.** Main mode between 300 and 500 s.

| Star | Modes (s) | Amp (mma) | $T_{\rm eff}$ (K) | $M$ ($M_\odot$) | Reference |
|---|---|---|---|---|---|
| WD J0916+3855 | 485.1 | 32.9 | 11 410 ± 50 | 0.67 ± 0.02 | Castanheira et al. (2007) |
| | 447.7 | 14.4 | | | |
| | 238.1 | 10.8 | | | |
| | 747.2 | 9.1 | | | |
| WD J1015+5954 | 401.7 | 20.8 | 11 630 ± 110 | 0.62 ± 0.04 | Mukadam et al. (2004) |
| | 453.7 | 15.8 | | | |
| | 1116.5 | 12.6 | | | |
| | 213.0 | 9.8 | | | |
| | 292.4 | 8.5 | | | |
| MCT 0145−221 | 462.2 | 25 | 11 500 ± 200 | 0.69 ± 0.03 | Bergeron et al. (2004) |
| | 727.9 | 19 | | | |
| | 823.2 | 15 | | | |
| HS 0507+0434B | 355.8 | 24.0 | 11 630 ± 200 | 0.71 ± 0.03 | Bergeron et al. (2004) |
| | 446.2 | 13.9 | | | |
| | 555.3 | 16.6 | | | |
| | 743.4 | 7.6 | | | |
| WD J0911+0310 | 352 | 27.7 | 11 630 ± 130 | 0.68 ± 0.05 | Kepler et al. (2005b) |
| | 757 | 16.4 | | | |
| WD J0949−0000 | 365.2 | 17.7 | 11 180 ± 130 | 0.75 ± 0.07 | Mukadam et al. (2004) |
| | 516.6 | 16.2 | | | |
| | 711.6 | 6.0 | | | |
| | 213.3 | 6.0 | | | |
| | 634.2 | 5.1 | | | |
| HE 0344+1207 | 392.9 | 21.1 | 11 470 ± 200 | 0.78 ± 0.03 | Voss et al. (2006) |
| | 762.2 | 18.9 | | | |
| | 461.0 | 11.4 | | | |

*Notes*. First subgroup of ZZ Ceti stars with main mode between 300 and 500 s, with the spectroscopic mean $T_{\rm eff}$ is 11 480 ± 130 K and mass $M = 0.68 \pm 0.03\,M_\odot$. WD J0949−0000, because of its faintness, and HE 0344+1207, because of the uncertainty determination from photometry in mass, were not included in this average, but they are still in this list because their detected modes fall within this group.

**Table 17.** Detected modes for ZZ Ceti stars with main mode between 300 and 500 s.

| Modes (s) | Amp (mma) | Model modes ($\ell$, $k$) |
|---|---|---|
| 213.1 | 7.9 | 205.0 (1,2) |
| 238.1 | 10.8 | 236.9 (1,3) |
| 292.4 | 8.5 | 283.6 (1,4) |
| 355.9 | 22.9 | 357.9 (1,6) |
| 396.8 | 21.0 | 398.6 (1,7) |
| 456.2 | 16.1 | 446.1 (1,8) |
| 485.1 | 32.9 | 483.5 (1,9) |
| 516.6 | 16.2 | 521.6 (1,10) |
| 555.3 | 16.6 | 557.5 (1,11) |
| 634.2 | 5.1 | 638.0 (1,13) |
| 711.6 | 6.0 | 716.0 (1,15) |
| 747.9 | 14.2 | 753.3 (1,16) |
| 823.2 | 15.0 | 832.7 (1,18) |
| 1116.5 | 12.6 | 1110.1 (1,25) |

*Notes*. Average values for the modes detected for the stars listed in Table 16 and in plot 2, which were used for the seismological analysis, compared with the modes of the best model with $T_{\rm eff}$ = 11 400 K, $M = 0.69\,M_\odot$, $M_{\rm H} = 10^{-4}\,M_*$ and $M_{\rm He} = 10^{-2}\,M_*$.

### 2.9 Main period between 500 and 700 s

Zuckerman & Becklin (1987) found a red excess in the photometry of G29−38. The most accepted hypothesis is a dust disc around the star (von Hippel et al. 2007), probably from a comet or small body disruption by tidal force. A similar disc has been observed for other white dwarfs (e.g. Jura, Farihi & Zuckerman 2007).

There are many simultaneously excited modes, which interfere with each other; in some runs, G29−38 pulsation amplitude was much lower than average (Winget et al. 1990). The main difficulty is to identify which are the real modes and which periodicities are linear combinations and harmonics. Our criterion was that if the parent modes are not present, frequencies coinciding with the daughter modes are assumed to be real.

In Table 21, we list the mean values of the modes from different observing campaigns from 1985 to 1993, from Kleinman et al. (1998), and the spectral determinations for temperature and mass. All spectroscopic temperatures are much hotter than expected for a red edge pulsator, which we would expect from its pulsational spectra.

Comparing the observed modes of G29−38 with the models, we found that the best seismological solution is $T_{\rm eff}$ = 11 700 K, $M = 0.665\,M_\odot$, $M_{\rm He} = 10^{-2}\,M_*$ and a thin $M_{\rm H} = 10^{-8}\,M_*$. It was a nice surprise that seismology gave a hot temperature, consistent with the spectroscopic determination, while our prejudice about

**Table 18.** Main mode between 300 and 500 s.

| Star | Modes (s) | Amp (mma) | $T_{\rm eff}$ (K) | $M$ ($M_{\odot}$) | Reference |
|---|---|---|---|---|---|
| G207−9 | 259.1 | 17.3 | 11 950 ± 200 | 0.83 ± 0.03 | Bergeron et al. (2004) |
| | 292.0 | 49.0 | 11 910 ± 170 | 0.77 ± 0.13 | Koester & Allard (2000) |
| | 318.0 | 64.0 | | | |
| | 557.4 | 63.4 | | | |
| | 740.7 | 46.4 | | | |
| WD J0815+4437 | 258.3 | 6.2 | 11 620 ± 170 | 0.57 ± 0.05 | Mukadam et al. (2004) |
| | 311.7 | 22 | | | |
| | 551.5 | 7.3 | | | |
| | 787.5 | 6.6 | | | |

*Notes*. ZZ Ceti stars with main mode between 300 and 500 s.

**Table 19.** Mean values for the modes of G207−9 and WD J0815+4437.

| Modes (s) | Amp (mma) |
|---|---|
| 259.0 | 11.8 |
| 292.0 | 33 |
| 317.3 | 43.0 |
| 557.3 | 35.4 |
| 740.7 | 27 |
| 787.5 | 24 |

*Notes*. Average values for the detected modes for the stars G207−9 and WD J0815+4437 listed in Table 18 and in Fig. 3, which were used for the seismological analysis.

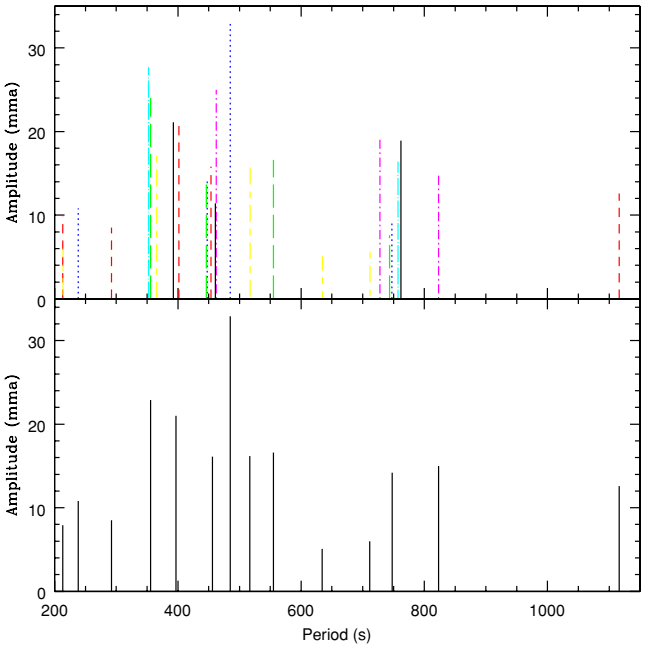


**Figure 2.** Upper panel: detected modes for the stars listed in Table 16. The (blue) dotted lines are the modes of the star WD J0916+3855, the (red) dashed lines of WD J1015+5951, the (magenta) dot–dashed lines of MCT 0145−221, the (green) long-dashed lines of HS 0507+0434B, the (cyan) long-dash–dotted lines of WD J0911+0310, the (yellow) long-short-dashed lines of WD J0949−0000 and the (black) full line of HE 0344+1207. Lower panel: average values of the modes for these stars, listed in Table 17, which we used for seismology.

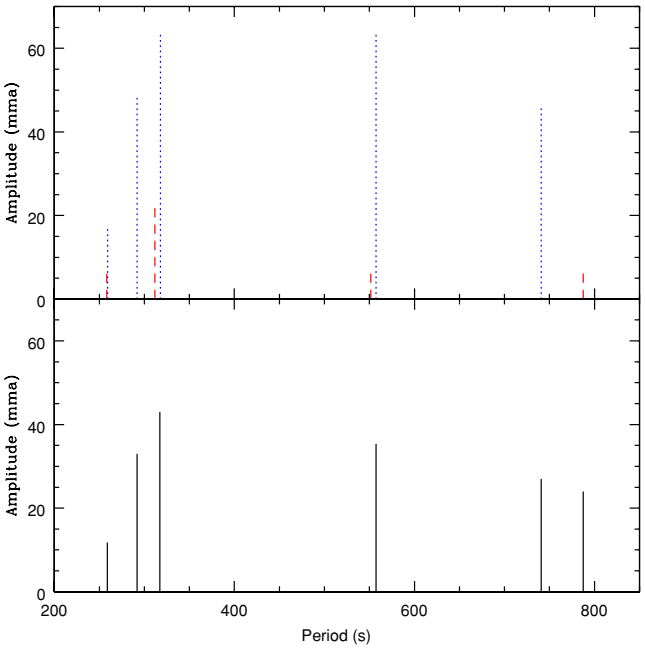


**Figure 3.** Upper panel: detected modes for the stars listed in Table 18. The (blue) dotted lines are the modes of the star G207−9 and the (red) dashed lines for WD J0851+4437. Lower panel: average values for the modes for these stars, listed in Table 19, which were used for seismology.

a cooler temperature was wrong. In Fig. 5, we show the comparison between the mean observed modes ($x$-axis) and the modes present in the best model ($y$-axis).

Kleinman et al. (1998) also studied seismologically G29−38 and found H layer mass should be $5 \times 10^{-7}\, M_{*}$, consistent with our determinations, as our uncertainty is around 0.5 dex.

The other stars that belong to this group are listed in Tables 22 and 23. As they were not observed in many campaigns, very little is known about all the modes that are excited in these stars. In Fig. 6, we plot all present modes in all stars with main mode between 500 and 700 s (upper panel). The mean values for the closest modes are shown in the lower panel and listed in Table 24.

We have not found a model within the entire grid with all these modes simultaneously, for $\ell = 1$ or 2. Our conclusion is that these stars must have different internal structures. In the red edge of the ZZ Ceti instability strip, all the modes can be excited, as predicted by theory, which makes it extremely difficult to find similarities among those stars. In Fig. 6, we also compare the detected modes with a model for the mean values of temperature (11 300 K) and

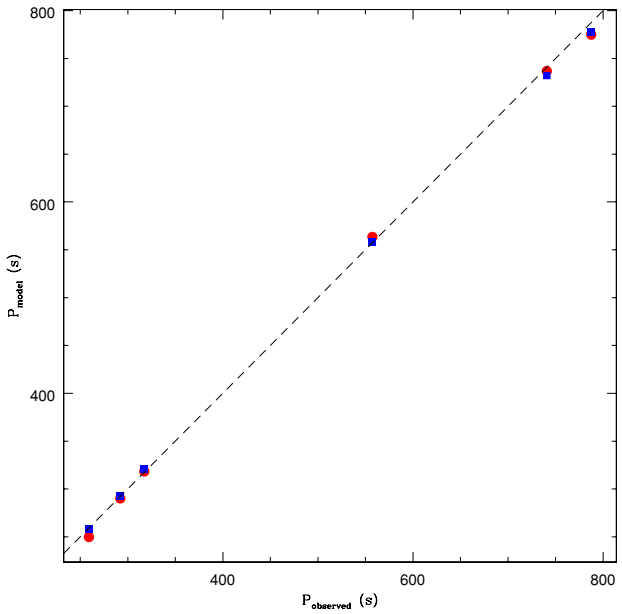


**Figure 4.** Comparison between the observed modes ($x$-axis) and the calculated ($y$-axis) for a model with $T_{\rm eff} = 12\,000$ K, $M = 0.815\,{\rm M}_{\odot}$, $M_{\rm H} = 10^{-8.5}\,M_{*}$ and $M_{\rm He} = 10^{-2}\,M_{*}$, identified by (red) circles, for the stars G207−9 and WD J0815+4437. The model identified by the (blue) squares has $T_{\rm eff} = 11\,700$ K, $M = 0.53\,{\rm M}_{\odot}$, $M_{\rm H} = 10^{-6.5}\,M_{*}$ and $M_{\rm He} = 10^{-3.5}\,M_{*}$, which is the low-mass solution. The dashed line shows the 1:1 correspondence between the observations and the fits. This degeneracy in solutions is an example of the core–envelope symmetry discussed by Montgomery (2005b).

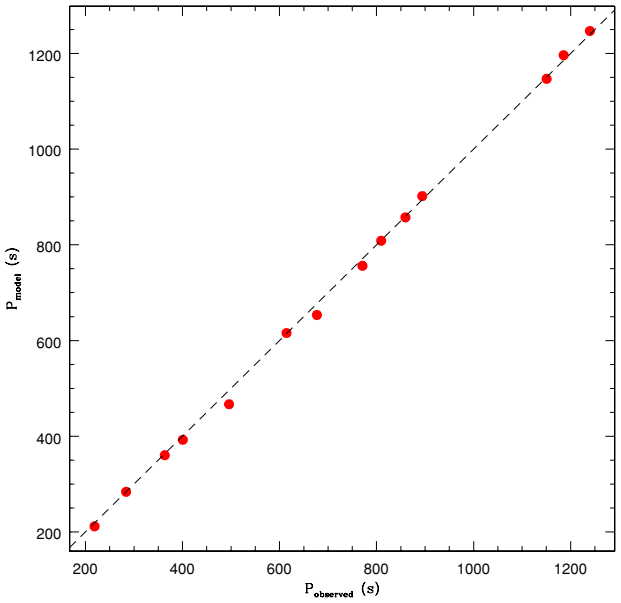


**Figure 5.** Comparison between the observed modes ($x$-axis) and the calculated ($y$-axis) for the model with $T_{\rm eff} = 11\,400$ K, $M = 0.675\,{\rm M}_{\odot}$, $M_{\rm H} = 10^{-8}\,M_{*}$ and $M_{\rm He} = 10^{-2}\,M_{*}$, identified by the (red) circles, for the star G29−38.

mass ($0.80\,{\rm M}_{\odot}$) and the canonic values of H and He layer, $10^{-4}$ and $10^{-2}\,M_{*}$, respectively. The lower sequence of dots represents the $\ell = 1$ modes present in the model and the upper sequence, the $\ell = 2$ modes.

**Table 20.** Main modes between 300 and 500 s.

| Star | Modes (s) | Amp (mma) | $T_{\rm eff}$ (K) | $M$ ($\rm M_{\odot}$) | Reference |
|---|---|---|---|---|---|
| WD J1355+5454 | 324.0 | 21.8 | 11 580 ± 140 | 0.58 ± 0.05 | Mullally et al. (2005) |
| WD J0851+0605 | 326 | 22.4 | 11 310 ± 50 | 0.68 ± 0.02 | Kepler et al. (2005b) |
| WD J1650+3010 | 339.1 | 14.7 | 11 100 ± 90 | 1.07 ± 0.04 | Castanheira et al. (2006) |
| WD J1310−0159 | 349.6 | 17.6 | 10 990 ± 70 | 0.57 ± 0.05 | Kepler et al. (2005b) |
| | 280 | 9.2 | | | |
| WD J1222−0243 | 396 | 22 | 11 400 ± 40 | 0.83 ± 0.02 | Kepler et al. (2005b) |

*Notes*. Other ZZ Ceti stars with main mode between 300 and 500 s.

**Table 21.** List of modes detected for G29−38.

| Star | Modes (s) | Amp (mma) | $T_{\rm eff}$ (K) | $M$ ($\rm M_{\odot}$) | Reference |
|---|---|---|---|---|---|
| G29−38 | 614.4 | 32.8 | 11 820 ± 200 | 0.69 ± 0.03 | Bergeron et al. (2004) |
| | 809.4 | 30.1 | 11 510 ± 120 | 0.61 ± 0.06 | Koester & Allard (2000) |
| | 859.6 | 24.6 | | | |
| | 894.0 | 14.0 | | | |
| | 400.5 | 9.1 | | | |
| | 496.2 | 7.9 | | | |
| | 655.1 | 6.1 | | | |
| | 770.8 | 5.1 | | | |
| | 283.9 | 4.8 | | | |
| | 363.5 | 4.7 | | | |
| | 1150.5 | 3.6 | | | |
| | 1185.6 | 3.4 | | | |
| | 1239.9 | 1.9 | | | |
| | 218.7 | 1.5 | | | |

**Table 22.** Main mode between 500 and 700 s.

| Star | Modes (s) | Amp (mma) | $T_{\rm eff}$ (K) | $M$ ($M_{\odot}$) | Reference |
|---|---|---|---|---|---|
| WD J2135−0743 | 565.4 | 49.8 | 11 190 ± 120 | 0.45 ± 0.04 | Castanheira et al. (2006) |
| | 299.9 | 22.9 | | | |
| | 510.6 | 16.8 | | | |
| | 281.8 | 13.3 | | | |
| | 323.2 | 13.0 | | | |
| EC 14012−1446 | 610.4 | 54.3 | 11 900 ± 200 | 0.71 ± 0.03 | Bergeron et al. (2004) |
| | 769.1 | 51.7 | | | |
| | 722.9 | 22.9 | | | |
| | 530.1 | 16.7 | | | |
| | 398.9 | 12.1 | | | |
| | 937.2 | 11.0 | | | |
| | 678.6 | 7.6 | | | |
| | 1217.4 | 7.5 | | | |
| | 882.7 | 2.9 | | | |
| WD J0000−0046 | 611.4 | 23.0 | 10 880 ± 110 | 0.81 ± 0.06 | Castanheira et al. (2007) |
| | 584.8 | 15.9 | | | |
| | 601.4 | 9.0 | | | |
| WD J1711+6541 | 612.6 | 5.7 | 11 310 ± 40 | 1.00 ± 0.02 | Mukadam et al. (2004) |
| | 606.3 | 5.2 | | | |
| | 690.3 | 3.3 | | | |
| | 1186.6 | 3.3 | | | |
| | 1248.2 | 3.2 | | | |
| | 561.5 | 3.0 | | | |
| | 934.8 | 2.9 | | | |
| | 214.3 | 1.7 | | | |
| | 234.0 | 1.2 | | | |
| WD J2231+1346 | 627.0 | 26.3 | 11 080 ± 100 | 0.58 ± 0.04 | Castanheira et al. (2006) |
| | 619.7 | 26.3 | | | |
| | 707.5 | 17.1 | | | |
| | 382.4 | 14.6 | | | |
| | 548.7 | 13.7 | | | |
| WD J1502−0001 | 629.5 | 32.6 | 11 200 ± 120 | 0.61 ± 0.05 | Mukadam et al. (2004) |
| | 418.2 | 14.9 | | | |
| | 687.5 | 12.0 | | | |
| | 581.9 | 11.1 | | | |
| WD J0825+0329 | 640.2 | 5.2 | 11 800 ± 110 | 0.82 ± 0.03 | Kepler et al. (2005b) |
| | 704.1 | 3.7 | | | |
| | 657.4 | 4.4 | | | |
| WD J0942+5733 | 694.7 | 37.7 | 11 260 ± 70 | 0.78 ± 0.03 | Mukadam et al. (2004) |
| | 451.0 | 18.4 | | | |
| | 550.5 | 12.2 | | | |

*Notes*. ZZ Ceti stars with main mode between 500 and 700 s.

**Table 23.** Main mode between 500 and 700 s.

| Star | Modes (s) | Amp (mma) | $T_{\rm eff}$ (K) | $M$ ($M_{\odot}$) | Reference |
|---|---|---|---|---|---|
| BPM 30551 | 606.8 | 11.5 | 11 260 ± 200 | 0.75 ± 0.03 | Bergeron et al. (2004) |
| | 744.7 | 10.5 | | | |
| KUV 08368+4026 | 618.0 | 16 | 11 490 ± 200 | 0.64 ± 0.03 | Bergeron et al. (2004) |
| | 494.5 | 5.5 | | | |
| WD J1618−0023 | 644.0 | 5.4 | 10 860 ± 160 | 0.71 ± 0.08 | Castanheira et al. (2006) |
| WD J0825+4119 | 653.4 | 17.1 | 11 820 ± 170 | 0.92 ± 0.04 | Mukadam et al. (2004) |
| | 611.0 | 11.2 | | | |
| HS 0733+4119 | 656.2 | 38.7 | 11 160 ± 200 | 0.47 ± 0.05 | Voss et al. (2006) |
| | 468.8 | 19.4 | | | |

*Notes*. Continuation of Table 22: ZZ Ceti stars with main mode between 500 and 700 s.

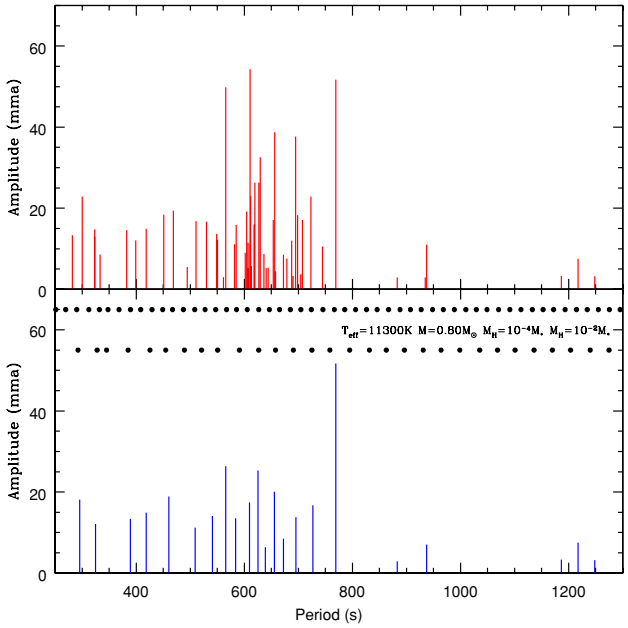


**Figure 6.** Upper panel: detected modes for the stars listed in Tables 22 and 23. Lower panel: mean mode values for these stars, listed in Table 24. The black dots indicate the present modes in a model with $T_{\rm eff} = 11\,300$ K, $M = 0.80\,{\rm M}_{\odot}$ and the canonic values for H and He layers equals to $10^{-4}$ and $10^{-2}\,M_{*}$, respectively. The lower dots are for $\ell = 1$ modes and the upper for $\ell = 2$.

**Table 24.** Mean values for the modes if the main mode is between 500 and 700 s, listed in Tables 22 and 23 and plotted in Fig. 6.

| Modes (s) | Amp (mma) |
|---|---|
| 220.9 | 1.5 |
| 295.3 | 18.1 |
| 324.8 | 12.1 |
| 389.1 | 13.4 |
| 418.2 | 14.9 |
| 460.4 | 18.9 |
| 509.0 | 11.2 |
| 540.7 | 14.1 |
| 565.4 | 26.4 |
| 583.8 | 13.5 |
| 609.7 | 17.4 |
| 625.3 | 25.3 |
| 638.9 | 6.4 |
| 655.8 | 20.1 |
| 672.3 | 8.5 |
| 695.2 | 13.8 |
| 726.7 | 16.7 |
| 769.1 | 51.7 |
| 882.7 | 2.9 |
| 937.0 | 7.0 |
| 1186.6 | 3.3 |
| 1217.4 | 7.5 |
| 1248.2 | 3.2 |

Because the stars in this group have different structure, they were studied separately and the minima in the families of seismological solutions are listed in Table 25.

For the stars with only one or two detected modes, we could not find a unique solution from seismology. Future observations revealing more excited modes are fundamental to study these stars through seismology.

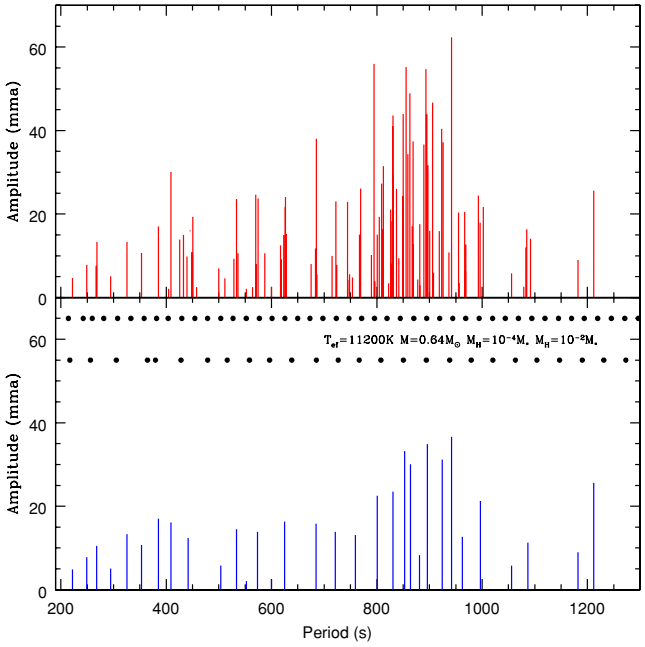


**Figure 7.** Upper panel: detected modes for the stars listed in Tables 26 and 27. Lower panel: average values for the modes of these stars. The black dots represent the model with $T_{\rm eff} = 11\,200$ K, $M = 0.64\,{\rm M}_{\odot}$ and the canonic values for the H and He layers $10^{-4}$ and $10^{-2}\,M_{*}$, respectively. The lower points are the $\ell = 1$ modes and the upper, $\ell = 2$.

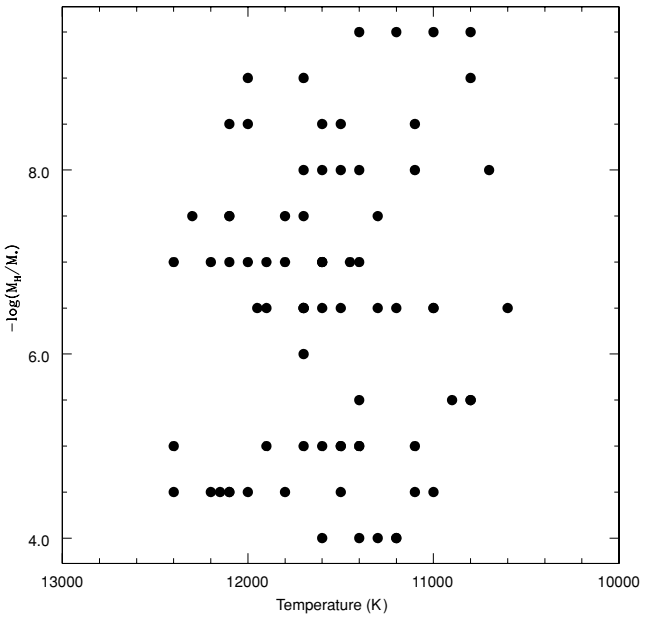


**Figure 8.** H mass versus $T_{\rm eff}$, showing that there is no evidence of accretion nor loss of the external layers, as the ZZ Ceti evolves in the instability strip. The uncertainty is the same for all the points.

### 2.10 ZZ Ceti stars in the red edge

The ZZ Ceti stars in the red edge (Tables 26 and 27) show that almost all the modes can be excited in this evolutionary phase. In Fig. 7, we show the average of the excited modes in comparison

**Table 25.** Seismology for ZZ Ceti stars with main mode between 500 and 700 s.

| Star | $T_{\rm eff}$ (K) | $M$ ($M_\odot$) | $-\log M_{\rm H}$ | $-\log M_{\rm He}$ | $S$ (s) | Modes ($\ell$, $k$) |
|---|---|---|---|---|---|---|
| WD J2135−0743 | 11 300 | 0.53 | 6.5 | 3.5 | 2.52 | 273.6(1,1), 295.1(1,2), 332.6(1,3) 530.7(1,6), 565.3(1,7) |
| EC 14012−1446 | 11 600 | 0.64 | 7.5 | 2.5 | 1.1 | 403.6(1,5), 532.9(1,17) 610.2(1,9), 663.1(1,10) 722.2(1,11), 770.3(1,13) 862.4(1,14), 916.6(1,15) 1216.2(1,21) |
| | 11 500 | 0.76 | 5 | 2.5 | 1.0 | 417.5(1,7), 529.3(1,10) 610.6(1,12), 687.5(1,14) 727.8(1,15), 769.1(1,16) 888.9(1,19), 927.1(1,20) 1204.0(1,27) |
| WD J0000−0046 | 10 600 | 0.705 | 8 | 2 | 2.34 | 579.8(1,8), 598.8(2,17), 612.4(1,9) |
| | 11 400 | 0.70 | 8 | 3 | 1.74 | 581.2(1,8), 597.2(2,17), 611.7(1,9) |
| WD J1711+6541 | 11 100 | 0.68 | 4 | 2 | 4.59 | 209.6(1,2), 242.2(1,3), 571.0(1,11) 609.2(1,12), 695.6(1,14), 935.9(1,20) 1176.7(1,26), 1255.8(1,28) |
| | 11 700 | 1.00 | 6 | 2.5 | 3.87 | 197.8(1,3), 234.7(1,4), 551.1(1,16) 607.0(1,18), 687.1(1,21), 934.9(1,30) 1188.9(1,39), 1244.7(1,41) |
| | 11 500 | 0.89 | 8 | 3.5 | 4.10 | 208.5(1,1), 230.7(1,2), 560.5(1,10) 599.5(1,11), 673.8(1,13), 923.4(1,19) 1173.0(1,25), 1260.0(1,27) |
| WD J2231+1346 | 10 600 | 0.625 | 4 | 2 | 3.33 | 380.8(1,5), 538.6(1,9) 622.0(1,11), 712.9(1,13) |
| | 10 800 | 0.64 | 8 | 2.5 | 2.98 | 378.6(1,4), 560.3(1,7) 624.2(1,8), 707.8(1,10) |
| | 10 600 | 0.56 | 7.5 | 3 | 3.42 | 371.1(1,3), 542.2(1,6) 623.2(1,7), 709.0(1,9) |
| | 11 600 | 0.62 | 8 | 3.5 | 2.60 | 384.8(1,3), 559.3(1,7) 622.8(1,8), 707.3(1,10) |
| WD J1502−0001 | 10 900 | 0.58 | 5.5 | 2.5 | 0.81 | 416.9(1,4), 576.3(1,7), 629.3(1,8) 684.2(1,9) |
| | 11 800 | 0.57 | 7 | 3.5 | 1.21 | 417.7(1,4), 586.3(1,7), 630.0(1,8) 695.2(1,9) |
| WD J0825+0329 | 11 300 | 0.785 | 4 | 2 | 1.4 | 638.8(1,14), 658.9(2,28) 704.6(1,16) |
| WD J0942+5733 | 11 200 | 0.76 | 4 | 2 | 0.62 | 448.7(1,8), 549.2(1,11), 694.4(1,15) |

*Notes*. Absolute minima in the possible families of solutions of the seismological analysis for the ZZ Ceti stars with main mode between 500 and 700 s.

with ones in the model for the mean values of $T_{\rm eff} = 11\,200$ K and $M = 0.64\,M_\odot$, and the canonic values for the H and He layers, $10^{-4}$ and $10^{-2}\,M_*$, respectively. Almost the full spectrum of modes is observed between ∼800 and ∼1000 s. Because of the asymptotic behaviour of high-$k$ modes, we analysed these stars separately. The minima of the possible families of solutions for each star are listed in Table 28.

Our main conclusion after studying this group is that there are some seismological solutions with extremely thin H layer, reaching $10^{-9.5}\,M_*$, our thinnest grid value.

The other stars of this group, with only two or even one detected mode, could not be studied by seismology, because there was not a unique solution. More modes need to be detected for these stars, or independent accurate temperature and mass determinations. In the red edge, different from what happens for the stars in the blue edge, few modes are not enough to study the interior of the stars.

### 2.11 ZZ Ceti stars stopping to pulsate

The final group of our study is the ZZ Ceti stars stopping to pulsate. They have long period and low-amplitude modes, as listed in Table 29. There are only two stars with three modes detected, for which it was possible to do seismology.

We started the analysis of this group by the star GD 154. This star was studied by Pfeiffer et al. (1996), who claimed that it has the thinnest H layer among all ZZ Ceti stars, $2 \times 10^{-10}\,M_*$. The most likely family of seismological solutions that agrees with the spectroscopic values (see Table 30) is consistent with their

**Table 26.** ZZ Ceti stars in the red edge.

| Star | Modes (s) | Amp (mma) | $T_{\rm eff}$ (K) | $M$ ($M_{\odot}$) | Reference |
|---|---|---|---|---|---|
| EC 0049−473 | 722 | 23 | | | Stobie et al. (1997) |
| | 867 | 17 | | | |
| | 1083 | 12 | | | |
| | 1182 | 9 | | | |
| | 500 | 7 | | | |
| HE 0532−560 | 723.7 | 7.8 | 11 560 ± 200 | 0.92 ± 0.03 | Fontaine et al. (2003) |
| | 686.1 | 5.5 | | | |
| | 753.8 | 4.8 | | | |
| | 822.3 | 3.4 | | | |
| | 881.7 | 2.9 | | | |
| | 599.7 | 2.5 | | | |
| | 563.7 | 2.5 | | | |
| | 522.4 | 2.1 | | | |
| HE 1258+0123 | 744.6 | 22.9 | 11 400 ± 200 | 0.63 ± 0.03 | Bergeron et al. (2004) |
| | 881.5 | 17.6 | 11 100 ± 30 | 0.68 ± 0.02 | Kepler et al. (2005b) |
| | 628.0 | 15.2 | | | |
| | 1092.1 | 14.1 | | | |
| | 439.2 | 9.8 | | | |
| | 528.5 | 9.3 | | | |
| WD J0906−0024 | 769.4 | 26.1 | 11 520 ± 90 | 0.61 ± 0.03 | Mukadam et al. (2004) |
| | 574.5 | 23.7 | | | |
| | 618.8 | 9.1 | | | |
| | 266.6 | 7.6 | | | |
| | 457.9 | 2.5 | | | |
| PG 2303+242 | 794.5 | 56 | 11 480 ± 200 | 0.66 ± 0.03 | Bergeron et al. (2004) |
| | 900.5 | 16 | | | |
| | 623.4 | 15 | | | |
| | 675.4 | 8 | | | |
| | 570.7 | 8 | | | |
| WD J1216+0922 | 830.9 | 43.6 | 11 290 ± 110 | 0.79 ± 0.05 | Kepler et al. (2005b) |
| | 409 | 30.1 | | | |
| | 570 | 24.6 | | | |
| | 626 | 21.6 | | | |
| | 967 | 20.5 | | | |
| WD J0318+0030 | 826.4 | 21.1 | 11 040 ± 70 | 0.65 ± 0.03 | Mukadam et al. (2004) |
| | 587.1 | 10.6 | | | |
| | 536.1 | 10.6 | | | |
| HE 1429−037 | 829.3 | 18.3 | 11 430 ± 40 | 0.52 ± 0.01 | Silvotti et al. (2005) |
| | 1084.9 | 16.3 | | | |
| | 969.0 | 12.7 | | | |
| | 450.1 | 10.2 | | | |
| R 808 | 907.6 | 5.9 | 11 160 ± 200 | 0.63 ± 0.03 | Bergeron et al. (2004) |
| | 511.3 | 4.6 | 10 900 ± 170 | 0.40 ± 0.08 | Koester & Allard (2000) |
| | 877.9 | 4.3 | | | |
| | 745.1 | 4.2 | | | |
| | 796.3 | 3.8 | | | |
| | 956.5 | 3.5 | | | |
| | 1079.1 | 2.6 | | | |
| | 404.5 | 2.1 | | | |
| HS 1625+1231 | 862.9 | 48.9 | 11 270 ± 300 | 0.6 ± 0.1 | Voss et al. (2006) |
| | 533.6 | 23.6 | | | |
| | 385.2 | 17.0 | | | |
| | 425.8 | 13.9 | | | |
| | 325.5 | 13.3 | | | |
| | 268.2 | 13.3 | | | |
| | 353.0 | 10.7 | | | |
| | 248.9 | 7.8 | | | |

**Table 26** – *continued*

| Star | Modes (s) | Amp (mma) | $T_{\rm eff}$ (K) | $M$ ($M_\odot$) | Reference |
|---|---|---|---|---|---|
| WD J2209−0919 | 894.7 | 43.8 | 11 430 ± 110 | 0.82 ± 0.06 | Castanheira (2007) |
| | 448.2 | 10.9 | | | |
| | 789.5 | 10.2 | | | |
| | 968.7 | 6.3 | | | |
| | 294.7 | 5.1 | | | |
| | 221.9 | 4.7 | | | |
| WD J1700+3549 | 893.4 | 54.7 | 11 160 ± 50 | 0.63 ± 0.03 | Mukadam et al. (2004) |
| | 955.3 | 20.4 | | | |
| | 450.5 | 19.3 | | | |
| WD J1255+0211 | 897 | 31.7 | 11 390 ± 150 | 0.71 ± 0.07 | Kepler et al. (2005b) |
| | 1002 | 21.7 | | | |
| | 812 | 16.4 | | | |
| WD J1157+0553 | 918.9 | 15.9 | 11 050 ± 50 | 0.70 ± 0.03 | Mukadam et al. (2004) |
| | 826.2 | 8.1 | | | |
| | 1056.2 | 5.8 | | | |
| | 748.5 | 5.6 | | | |
| WD J0102−0032 | 926.1 | 37.2 | 11 050 ± 100 | 0.76 ± 0.05 | Bergeron et al. (2004) |
| LP 586−051 | 830.3 | 29.2 | | | |
| EC 23487−2424 | 992.7 | 24.4 | 11 520 ± 200 | 0.67 ± 0.03 | Bergeron et al. (2004) |
| | 804.5 | 19.3 | | | |
| | 868.2 | 12.8 | | | |
| WD J2159+1322 | 801.0 | 15.1 | 11 710 ± 160 | 0.99 ± 0.04 | Mullally et al. (2005) |
| | 683.7 | 11.7 | | | |
| G225−2 | 830 | 41 | 11 440 ± 200 | 0.71 ± 0.03 | Bergeron et al. (2004) |
| | 685 | 38 | | | |
| WD J0855+0635 | 850 | 44 | 11 050 ± 50 | 0.88 ± 0.02 | Castanheira et al. (2006) |
| | 433 | 15 | | | |
| HS 1039+4112 | 855.5 | 55.2 | 11 550 ± 200 | 0.67 ± 0.03 | Gianninas et al.2005 |
| | 837.3 | 26 | | | |
| WD J1122+0358 | 859.0 | 34.3 | 11 070 ± 80 | 0.64 ± 0.04 | Mukadam et al. (2004) |
| | 996.1 | 17.9 | | | |
| WD J1054+5307 | 869.1 | 37.4 | 11 120 ± 80 | 0.61 ± 0.03 | Mullally et al. (2005) |
| | 444.6 | 16.0 | | | |
| WD J1617+4324 | 889.6 | 36.6 | 11 190 ± 100 | 0.63 ± 0.04 | Mukadam et al. (2004) |
| | 626.3 | 24.1 | | | |
| WD J1417+0058 | 894.5 | 44.0 | 11 300 ± 80 | 0.63 ± 0.03 | Mukadam et al. (2004) |
| | 812.5 | 31.5 | | | |
| WD J1106+0115 | 937 | 10.8 | 10 990 ± 60 | 0.66 ± 0.03 | Kepler et al. (2005b) |
| | 842 | 9.4 | | | |
| WD J2307−0847 | 1212.2 | 25.6 | 11 060 ± 110 | 0.73 ± 0.06 | Castanheira et al. (2006) |
| | 617.0 | 12.5 | | | |

**Table 27.** ZZ Ceti stars in the red edge with only one detected mode.

| Star | Modes (s) | Amp (mma) | $T_{\rm eff}$ (K) | $M$ ($M_\odot$) | Reference |
|---|---|---|---|---|---|
| WD J1337+0104 | 715 | 10.0 | 11 530 ± 160 | 0.95 ± 0.04 | Kepler et al. (2006) |
| WD J0332−0049 | 767.5 | 15.1 | 11 040 ± 70 | 0.77 ± 0.04 | Mukadam et al. (2004) |
| WD J1641+3521 | 809.3 | 27.3 | 11 240 ± 170 | 0.87 ± 0.06 | Eisenstein et al. (2006) |
| WD J1408+0445 | 849 | 24.3 | 10 940 ± 60 | 0.64 ± 0.03 | Kepler et al. (2005b) |
| WD J1257+0124 | 905.8 | 46.7 | 11 520 ± 160 | 0.86 ± 0.06 | Castanheira et al. (2006) |
| WD J2334+0103 | 923.2 | 40.4 | 11 400 ± 210 | 0.60 ± 0.08 | Castanheira et al. (2006) |
| WD J1056−0006 | 942.2 ($f_1$) | 62.3 | 11 020 ± 50 | 0.54 ± 0.02 | Mukadam et al. (2004) |
| | 474.4 ($2 \times f_1$) | 22.9 | | | |
| | 314.2 ($3 \times f_1$) | 11.0 | | | |
| KUV 02464+3239 | 831.6 | – | 11 290 ± 200 | 0.65 ± 0.03 | Fontaine et al. (2003) |

**Table 28.** Seismology for the ZZ Ceti stars in the red edge.

| Star | $T_{\rm eff}$ (K) | $M$ ($M_\odot$) | $-\log M_{\rm H}$ | $-\log M_{\rm He}$ | $S$ (s) | Modes ($\ell$, $k$) |
|---|---|---|---|---|---|---|
| WD J0906−0024 | 11 600 | 0.64 | 7.5 | 2 | 1.73 | 287.5(1,2), 480.4(1,6), 574.5(1,8) 610.2(1,9), 770.3(1,12) |
| | 11 600 | 0.64 | 7 | 3 | 0.90 | 270.9(1,2), 480.5(1,6), 575.5(1,8) 622.3(1,9), 770.1(1,12) |
| PG 2303+242 | 11 400 | 0.55 | 7 | 2.5 | 0.67 | 580.3(1,7), 623.5(1,8), 675.2(1,9) 794.8(1,11), 893.6(1,13) |
| | 10 800 | 0.66 | 9 | 3.5 | 0.63 | 574.9(1,7), 625.9(1,8), 694.5(1,9) 794.7(1,11), 895.4(1,13) |
| WD J1216+0922 | 11 500 | 0.69 | 5 | 2.5 | 2.03 | 407.4(1,5), 574.1(1,9), 619.1(1,10) 830.8(1,15), 963.0(1,18) |
| | 11 100 | 0.77 | 8.5 | 3 | 2.35 | 408.4(1,5), 564.1(1,8), 632.9(1,10) 830.7(1,14), 972.5(1,17) |
| WD J0318+0030 | 11 500 | 0.675 | 7 | 2 | 0.39 | 536.9(1,8), 586.4(1,9), 826.1(1,14) |
| | 10 800 | 0.65 | 5.5 | 2.5 | 0.31 | 536.9(1,7), 587.7(1,8), 826.2(1,13) |
| | 11 200 | 0.57 | 8.5 | 3.5 | 0.76 | 533.2(1,6), 587.5(1,7), 826.1(1,11) |
| HE 1429−037 | 11 400 | 0.69 | 9.5 | 2 | 3.45 | 445.3(1,5), 831.5(1,13) 974,8(1,16), 1081,3(1,18) |
| | 11 400 | 0.68 | 9.5 | 3.5 | 2.36 | 456.4(1,5), 826.9(1,12) 970,6(1,15), 1086,1(1,17) |
| WD J2209−0919 | 11 200 | 0.81 | 4 | 2 | 0.53 | 450.0(1,9), 786.4(1,19) 887.4(1,22), 988.7(1,25) |
| WD J1700+3549 | 11 100 | 0.64 | 8.5 | 3.5 | 0.62 | 451.6(1,5), 894.0(1,13), 954.3(1,14) |
| WD J1255+0211 | 11 200 | 0.67 | 9.5 | 2 | 1.18 | 807.2(1,12), 896.7(1,14), 1002.4(1,16) |
| | 11 700 | 0.70 | 7 | 3.5 | 1.69 | 805.0(1,13), 897.4(1,15), 1000.4(1,17) |
| WD J1157+0553 | 10 800 | 0.685 | 5.5 | 2 | 0.94 | 730.3(1,12), 813.4(1,14) 904.5(1,16), 1037.8(1,19) |
| EC 23487−2424 | 11 300 | 0.72 | 7.5 | 2 | 2.47 | 806.6(1,14), 858.5(1,15), 992,7(1,18) |
| HE 0532−560 | 11 000 | 0.695 | 4 | 2 | 3.30 | 526.2(1,10), 563.3(1,11), 600.0(1,12) 685.4(1,14), 722.7(1,15), 759.6(1,16) 839.0(1,18), 881.5(1,19) |
| | 11 400 | 0.97 | 5.5 | 3 | 1.86 | 527.4(1,13), 558.9(1,14), 595.0(1,15) 689.7(1,18), 723.3(1,19), 754.9(1,20) 818.7(1,22), 886.4(1,24) |
| HE 1258+0123 | 12 000 | 0.64 | 9 | 2 | 1.28 | 435.1(1,5), 520.9(1,7), 629.1(1,9) 744.5(1,11), 880.6(1,14), 1093.0(1,18) |
| | 11 500 | 0.71 | 9.5 | 3 | 2.01 | 440.6(1,5), 523.4(1,7), 628.1(1,9) 743.7(1,11), 878.7(1,14), 1088.1(1,18) |
| HS 1625+1231 | 11 000 | 0.785 | 4.5 | 2 | 1.69 | 227.7(1,3), 271.5(1,4), 327.9(1,5) 345.5(1,6), 377.5(1,7), 422.5(1,8) 529.3(1,11), 862.1(1,20) |
| WD J2209−0919 | 11 700 | 0.74 | 9 | 3 | 0.31 | 222.0(1,1), 300.8(1,2), 448.3(1,6) 789.6(1,13), 894.6(1,15), 982.5(1,17) |
| R 808 | 11 000 | 0.65 | 9.5 | 3.5 | 4.5 | 413.6(2,9), 513.9(1,6), 747.8(1,10) 794.8(2,21), 866.3(1,12), 908.6(1,13) 957.9(1,14), 1077.1(1,16) |

*Notes*. Absolute minima in the possible families of solutions in the seismological analysis for the typical ZZ Ceti stars in the red edge.

determination. However, there is yet another solution for H layer mass of $10^{-7.5}\,M_*$.

HS 0952+1816 mass determination, from photometry alone, has a high uncertainty. Our seismological study was able to lower this value from 0.2 to 0.13 $M_\odot$. As for GD 154, the H layer is very thin, $10^{-8}\,M_*$.

## 3 FINAL DISCUSSIONS AND CONCLUSIONS

There are many stars in the red edge that need to be re-observed with time-resolved photometry to detect more of the excited modes. This will allow us to study their interiors. We have demonstrated that it is possible to do seismology, even when a few modes are

**Table 29.** Pulsation modes of ZZ Ceti stars stopping to pulsate.

| Star | Modes (s) | Amp (mma) | $T_{\rm eff}$ (K) | $M$ ($M_\odot$) | Reference |
|---|---|---|---|---|---|
| GD 154 | 1186.5 | 2.4 | 11 180 ± 200 | 0.70 ± 0.03 | Bergeron et al. (2004) |
| | 1088.6 | 2.0 | | | |
| | 402.6 | 0.3 | | | |
| HS 0952+1816 | 1159.7 | 4.8 | 11 000 ± 500 | 0.4 ± 0.2 | Homeier & Koester (2001) |
| | 1466.0 | 4.5 | | | |
| | 853.8 | 3.9 | | | |
| WD J0303−0808 | 707 | 4.1 | 11 400 ± 110 | 0.92 ± 0.04 | Castanheira et al. (2006) |
| | 1128 | 3.5 | | | |
| G232−38 | 984.0 | 2.2 | 11 350 ± 200 | 0.61 ± 0.03 | Gianninas et al. (2006) |
| | 1147.5 | 1.9 | | | |
| | 741.6 | 1.9 | | | |
| WD J1443+0134 | 968.9 | 7.5 | 11 830 ± 150 | 0.7 ± 0.1 | Mukadam et al. (2004) |
| | 1085.0 | 5.2 | | | |
| WD J0249−0100 | 1045.3 | 8.9 | 11 060 ± 110 | 0.80 ± 0.06 | Castanheira et al. (2006) |
| | 1006.5 | 8.6 | | | |
| WD J0843+0431 | 1049 | 11.4 | 11 250 ± 60 | 0.72 ± 0.03 | Kepler et al. 2005 |
| | 1085 | 7.42 | | | |
| G30−20 | 1068 | 13.8 | 11 000 ± 100 | 0.92 ± 0.06 | Mukadam et al. (2002) |
| | | | 11 070 ± 200 | 0.58 ± 0.02 | Bergeron et al. (2004) |
| EC 13429−2342 | 1177.0 | 6.2 | 10 910 ± 300 | 0.60 ± 0.05 | Voss et al. (2006) |
| | 982.0 | 5.17 | | | |
| WD J1732+5905 | 1248.4 | 22.5 | 10 860 ± 100 | 0.60 ± 0.04 | Mukadam et al. (2004) |
| | 1122.4 | 10.2 | | | |
| PG 1149+058 | 1023.5 | 10.5 | 10 980 ± 300 | 0.64 ± 0.05 | Voss et al. (2006) |
| MCT 0016−2553 | 1152.4 | 8.1 | 10 900 ± 200 | 0.63 ± 0.05 | Gianninas et al. (2005) |
| GD 1212 | 1160.7 | 5.4 | 11 040 ± 200 | 0.67 ± 0.03 | Gianninas et al. (2005) |
| HS 0235+069 | 1238.7 | 4.7 | 11 000 ± 500 | 0.5 ± 0.2 | Homeier & Koester (2001) |
| GD 99 | 1311 | 5 | 11 820 ± 200 | 0.66 ± 0.03 | Bergeron et al. (2004) |
| KUV 03442+0719 | 1348.9 | 7.6 | 10 930 ± 200 | 0.51 ± 0.03 | Gianninas et al. (2006) |
| WD 1959+059 | 1350.4 | 5.7 | 11 030 ± 300 | 0.75 ± 0.05 | Voss et al. (2006) |

*Notes*. ZZ Ceti stars with pulsation mode representatives of when the stars are stopping to pulsate.

**Table 30.** Seismology of ZZ Ceti stars stopping to pulsate.

| Star | $T_{\rm eff}$ (K) | $M$ ($M_\odot$) | $-\log M_{\rm H}$ | $-\log M_{\rm He}$ | $S$ (s) | Modes ($\ell$, $k$) |
|---|---|---|---|---|---|---|
| GD 154 | 11 200 | 0.68 | 7.5 | 2 | 0.30 | 398.2(1,5), 1088.5(1,19), 1186.9(1,21) |
| | 10 800 | 0.73 | 9.5 | 2.5 | 0.11 | 396.9(1,4), 1088.5(1,18), 1186.5(1,20) |
| HS 0952+1816 | 10 700 | 0.52 | 8 | 2.5 | 1.74 | 856.6(1,11), 1161.3(1,16) 1465.1(1,21) |
| | 10 700 | 0.53 | 8 | 3 | 1.77 | 855.0(1,11), 1160.5(1,16) 1463.3(1,21) |

*Notes*. Absolute minima in the possible families of solutions of the seismological analysis for the ZZ Ceti stars stopping to pulsate.

detected and/or reliable temperature and mass are available, with a minimum of four parameters. More precise spectroscopy will allow better determinations of the atmospheric parameters of the faint stars, providing two extra measurements. For many years, the red edge stars relegated to oblivion, because we did not know how to study them.

Another important conclusion is that the H layer mass is not dependent on temperature (see Fig. 8), according to

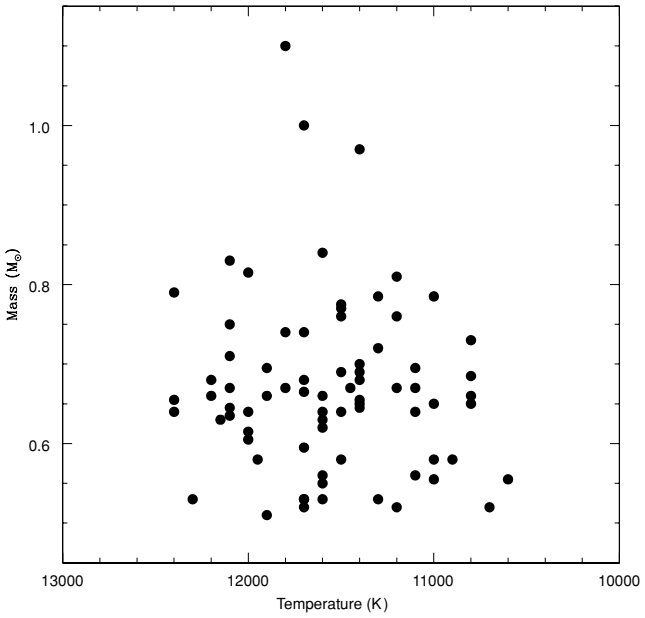


**Figure 9.** ZZ Ceti instability strip derived from seismology of these stars. We have included just the best solution for each studied star.

Kolmogorov–Smirnov and correlation of coefficients tests. Therefore, there is no evidence for accretion or loss of the external layers, as it happens for Miras, e.g., as the H layer mass does not vary univocally with temperature (or age). The mass loss of the external layer could come from the lack of reflectivity of the wave in the external layers, as calculated by Hansen, Winget & Kawaler (1985).

The mean value for the H layer mass is $10^{-6.3\pm1.6}\,M_*$, which is different than the canonical value of $10^{-4}\,M_*$, from evolutionary calculations. This result indicates that some white dwarfs, even if their masses are near the most probable value, might have formed with H mass several orders of magnitude smaller than the value predicted by the theory, i.e. it is probable that the mass loss during their evolution was, in fact, more efficient than assumed by the models. These results are preliminary and do not include the possible effects of realistic C/O profiles on the fits.

Using the seismological results, we derived an autoconsistent instability strip (see Fig. 9), which includes the stars from the bright sample and the SDSS stars. This is the first time that almost all known ZZ Ceti stars are studied as a group by seismology.

We have done the first large seismological analysis of the ZZ Ceti stars as a group, studying 83 stars; before only 12 ZZ Ceti stars had been studied seismologically. Even though we used the spectroscopic determinations as a guide, we only restricted the seismological solution to the range of spectroscopic parameters if there were not enough modes detected, avoiding local minima to be mistaken as global. In our study, we used the observed amplitudes as weights for the modes in the fits. It is not acceptable that the best fit does not agree with the highest amplitude mode. After 40 years since the discovery of the first ZZ Ceti star (Landolt 1968), we finally extracted information about this class as a whole.

Our seismological study of the ZZ Ceti stars is the proof that seismology is really a powerful tool in the study of stellar evolution. Even for the stars with few excited modes, it is possible to determine some characteristic of its interior. If in the blue edge, as R 548, many parameters could be determined, because the modes are not asymptotic. In the case of G29−38, we thought that the spectroscopic solutions were wrong, but we have obtained the same temperature and mass from our seismological study. It was a nice surprise that spectroscopy was right, agreeing with seismology, and that our prejudice that G29−38 should be in the red edge was wrong.

## ACKNOWLEDGMENTS

We acknowledge support from the CNPq-Brazil. This work has been done with observations from the SOAR telescope, a collaboration among CNPq-Brazil, NOAO, UNC and MSU.

## REFERENCES

Bergeron P., Wesemael F., Lamontagne R., Fontaine G., Saffer R. A., Allard N. F., 1995, ApJ, 449, 258
Bergeron P., Fontaine G., Billères M., Boudreault S., Green E. M., 2004, ApJ, 600, 404
Bischoff-Kim A., Montgomery M. H., Winget D. E., 2008, ApJ, 675, 1512
Bradley P. A., 2001, ApJ, 552, 326
Brickhill A. J., 1991, MNRAS, 252, 334
Castanheira B. G., 2007, PhD thesis, UFRGS, Brazil
Castanheira B. G., Kepler S. O., 2008, MNRAS, 385, 430 (Paper I)
Castanheira B. G. et al., 2006, A&A, 450, 227
Castanheira B. G. et al., 2007, A&A, 462, 989
Córsico A. H., Benvenuto O. G., Althaus L. G., Isern J., García-Berro E., 2001, New Astron., 6, 197
Córsico A. H., Althaus L. G., Kepler S. O., Costa J. E. S., Miller Bertolami M. M., 2008, A&A, 478, 869
Costa J. E., 2004, PhD thesis, UFRGS, Brazil
Eisenstein D. J. et al., 2006, ApJS, 167, 40
Fontaine G., Brassard P., Bergeron P., 2001, PASP, 113, 409
Fontaine G., Bergeron P., Billères M., Charpinet S., 2003, ApJ, 591, 1184
Gianninas A., Bergeron P., Fontaine G., 2005, ApJ, 631, 1100
Gianninas A., Bergeron P., Fontaine G., 2006, AJ, 132, 831
Giovannini O., Kepler S. O., Kanaan A., Wood A., Claver C. F., Koester D., 1998, Balt. Astron., 7, 131
Hansen B. M. S., Liebert J., 2003, ARA&A, 41, 465
Hansen C. J., Winget D. E., Kawaler S. D., 1985, ApJ, 297, 544
Homeier D., Koester D., 2001, in Provencal J. L., Shipman H. L., MacDonald J., Goochild S., eds, ASP Conf. Ser. Vol. 226, 12th European Workshop on White Dwarfs. Astron. Soc. Pac., San Francisco, p. 397
Jura M., Farihi J., Zuckerman B., 2007, ApJ, 663, 1285
Kanaan A. et al., 2005, A&A, 432, 219
Kepler S. O. et al., 2005a, ApJ, 634, 1311
Kepler S. O., Castanheira B. G., Saraiva M. F. O., Nitta A., Kleinman S. J., Mullally F., Winget D. E., Eisenstein D. J., 2005b, A&A, 442, 629
Kepler S. O., Castanheira B. G., Costa A. F. M., Koester D., 2006, MNRAS, 372, 1799
Kepler S. O., Kleinman S. J., Nitta A., Koester D., Castanheira B. G., Giovannini O., Costa A. F. M., Althaus L., 2007, MNRAS, 375, 1315
Kleinman S. J. et al., 1998, ApJ, 495, 424
Kleinman S. J. et al., 2004, ApJ, 607, 426
Koester D., Allard N. F., 2000, Balt. Astron., 9, 119
Koester D. et al., 2001, A&A, 378, 556
Landolt A. U., 1968, ApJ, 153, 151
Metcalfe T. S., 2005, MNRAS, 363, L86
Montgomery M. H., 2005a, ApJ, 633, 1142
Montgomery M. H., 2005b, in Koester D., Moehler S., eds, ASP Conf. Ser. Vol. 334, 14th European Workshop on White Dwarfs. Astron. Soc. Pac., San Francisco, p. 553
Mukadam A. S., Kepler S. O., Winget D. E., Bergeron P., 2002, ApJ, 580, 429
Mukadam A. S. et al., 2004, ApJ, 607, 982
Mukadam A. S., Montgomery M. H., Winget D. E., Kepler S. O., Clemens J. C., 2006, ApJ, 640, 956
Mullally F., Thompson S. E., Castanheira B. G., Winget D. E., Kepler S. O., Eisenstein D. J., Kleinman S. J., Nitta A., 2005, ApJ, 625, 966

Mullally F., Winget D. E., Degennaro S., Jeffery E., Thompson S. E., Chandler D., Kepler S. O., 2008, ApJ, 676, 573
O'donoghue D. E., Warner B., 1982, MNRAS, 200, 563
Pfeiffer B. et al., 1996, A&A, 314, 182
Silvotti R., Voss B., Bruni I., Koester D., Reimers D., Napiwotzki R., Homeier D., 2005, A&A, 443, 195
Stobie R. S., Kilkenny D., Koen C., O'Donoghue D., 1997, in Philip A. G. D., Liebert J., Saffer R., Hayes D. S., eds, The Third Conference on Faint Blue Stars. Contribution of the Institute for Space Observations No. 16. L. Davis Press, p. 497
von Hippel T., Kuchner M. J., Kilic M., Mullally F., Reach W. T., 2007, ApJ, 662, 544
Voss B., Koester D., Østensen R., Kepler S. O., Napiwotzki R., Homeier D., Reimers D., 2006, A&A, 450, 1061
Winget D. E. et al., 1990, ApJ, 357, 630
Winget D. E. et al., 2003, ASP Conf. Ser. 294, Scientific Frontiers in Research on Extrasolar Planets. Astron. Soc. Pac., San Francisco, p. 59
Winget D. E., Sullivan D. J., Metcalfe T. S., Kawaler S. D., Montgomery M. H., 2004, ApJ, 602, L109
Zuckerman B., Becklin E. E., 1987, Nat, 330, 138

This paper has been typeset from a TEX/LATEX file prepared by the author.